Cell Reports
Medicine

Article

Corticostriatal circuits in the transition to chronic back pain: The predictive role of reward learning

Graphical abstract

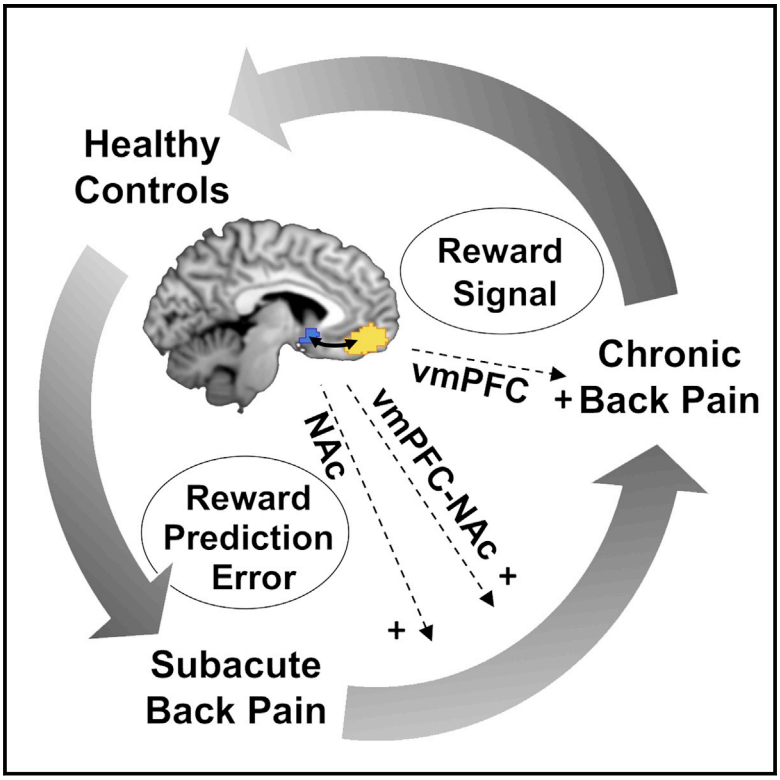

Highlights

- Frontostriatal circuits of reward learning predict distinct stages of back pain
- Frontostriatal prediction error signals predict chronic back pain
- Frontal encoding of reward signals characterizes the chronic stage of back pain

Authors

Martin Löffler, Seth M. Levine, Katrin Usai, Simon Desch, Mina Kandić, Frauke Nees, Herta Flor

Correspondence

martin.loeffler@zi-mannheim.de

In brief

Corticostriatal pathways contribute to the development of chronic back pain. In this issue of *Cell Reports Medicine*, Löffler et al. demonstrate that reward-learning signals in a prefrontal-limbic pathway predict the transition from subacute to chronic back pain and characterize the chronic stage of back pain.

Löffler et al., 2022, Cell Reports Medicine *3*, 100677
July 19, 2022
https://doi.org/10.1016/j.xcrm.2022.100677

CellPress

Cell Reports Medicine

CellPress
OPEN ACCESS

Article

Corticostriatal circuits in the transition to chronic back pain: The predictive role of reward learning

Martin Löffler,[1,5,*] Seth M. Levine,[1,2] Katrin Usai,[1] Simon Desch,[1] Mina Kandić,[1] Frauke Nees,[1,3,4] and Herta Flor[1,4]

[1]Institute of Cognitive and Clinical Neuroscience, Central Institute of Mental Health, Medical Faculty Mannheim, Heidelberg University, Square J5, 68159 Mannheim, Germany

[2]Department of Psychology, Ludwig Maximilian University Munich, Munich, Germany

[3]Institute of Medical Psychology and Medical Sociology, University Medical Center Schleswig Holstein, Kiel University, Kiel, Germany

[4]These authors contributed equally

[5]Lead contact

*Correspondence: martin.loeffler@zi-mannheim.de

https://doi.org/10.1016/j.xcrm.2022.100677

SUMMARY

Connectivity between the nucleus accumbens (NAc) and ventromedial prefrontal cortex (vmPFC) and reward learning independently predict the transition from acute to chronic back pain (CBP). However, how these predictors are related remains unclear. Using functional magnetic resonance imaging, we investigate NAc- and vmPFC-dependent reward learning in 50 patients with subacute back pain (SABP) and follow them over 6 months. Additionally, we compare 29 patients with CBP and 29 pain-free controls to characterize mechanisms of reward learning in the chronic stage. We find that the learning-related updating of the value of reinforcement (prediction error) in the NAc predicts the transition to chronicity. In CBP, compared with controls, vmPFC responses to this prediction error signal are decreased, but increased during a discriminative stimulus. Distinct processes of reward learning in the vmPFC and NAc characterize the development and maintenance of CBP. These could be targeted for the prevention and treatment of chronic pain.

INTRODUCTION

Chronic pain is a debilitating health problem, and its treatment and prevention are central challenges to the healthcare system. Identifying predictors of chronic pain is essential for its prevention, and learning is widely accepted as a major factor driving the development and maintenance of primary chronic pain.[1,2] More than 50 years ago, Fordyce[3] proposed that operant conditioning, defined as the learning of associations between behaviors and their consequences, instigates and maintains disabling pain behaviors and thus chronicity. Since then, several studies empirically supported a relationship between maladaptive behaviors in patients with chronic pain and positive and negative reinforcement, i.e., by the appearance of desired consequences or the removal of undesired consequences following maladaptive behaviors[4–7] as well as their role in the transition to chronic pain.

On the other hand, major contributions have been made to understand the brain mechanisms that mediate the transition from acute to chronic pain. In patients with subacute back pain (SABP), Baliki et al.[8] reported that increased functional prefrontal-limbic (ventromedial prefrontal cortex [vmPFC]-nucleus accumbens [NAc]) connectivity during phases of high ongoing pain predicted the transition to chronic pain after 12 months.

This vmPFC-NAc circuit was previously described as a common pathway of pain, reward processing, and reward learning.[9,10] More specifically, human,[11,12] as well as rodent,[13,14] studies showed that the NAc encodes prediction error signals during reward learning, based on the difference between expected rewards and reward feedback.[15] These predicted rewards may be positive reinforcers such as food but also pain relief as a negative reinforcer.[16] The vmPFC mainly encodes discriminative stimuli during reward learning,[17] i.e., stimuli that precede operant behavior and increase or decrease the likelihood for the respective behavior to occur. It also encodes the expectation of positive events such as monetary rewards, pleasant narratives, food rewards, or relief from a heat-pain stimulus.[9,18]

Interestingly, the response of the NAc to positive and negative reinforcers changes during the development of chronic pain. While rats showed enhanced dopamine levels in the NAc during pain relief as well as food reward 17 to 20 days after spinal nerve ligation (SNL), no such response was reported 31 to 34 days[19] later. Such brain changes in early pain stages have been linked to maladaptive emotional learning;[20,21] however, to what extent learning processes contribute to alterations in this corticolimbic circuit and thereby lead into chronicity needs to be examined.

Brain changes in chronic back pain include reduced gray matter volume in the vmPFC[22] and the NAc, a loss of low-frequency

fluctuation in the NAc,[23] and a decline in functional resting-state connectivity between the vmPFC and other brain regions, including the NAc,[24] which was related to increased behavioral preference for monetary rewards compared with pain relief.[25] Further, patients with chronic back pain (CBP) showed impaired reward learning in the Iowa gambling task compared with controls, and the number of perseverative errors during a modified version of the Wisconsin card-sorting test increased with pain duration.[26] Further, patients with fibromyalgia showed reduced vmPFC responses to reward anticipation,[27] but it is unknown so far if this extends to more localized CBP.

In summary, the vmPFC-NAc circuit plays a critical role during reward learning by updating the association between behavior and consecutive rewards (NAc) and by encoding anticipated reward values and tracking the predictive value of environmental/discriminative stimuli (vmPFC). These processes seem to be differentially affected in early and late phases of the development of chronic pain: while the chronic stage is characterized by enhanced vmPFC responses to established signals in anticipation of reward, the early stage seems to be characterized by overemphasizing the exploration of reward feedback. In other words, there seems to be a shift from exploration to exploitation during the development of CBP, but it is unclear if this exploration-exploitation dilemma predicts the development of chronic pain.

We therefore sought to determine to what extent operant-learning processes that are encoded in the vmPFC-NAc pathway may explain the transition from subacute to CBP as well as the maintenance of CBP. We hypothesized that increases of the NAc response to reward prediction error signals predict the development of chronic pain in patients with SABP, whereas the chronic stage of back pain is characterized by reduced vmPFC responses during reward expectation and in response to discriminative stimuli. To test these hypotheses, we carried out task-based functional magnetic resonance imaging (fMRI) during an instrumental conditioning paradigm with money and pain relief as positive and negative reinforcers (see Figure 1). We followed up with patients with SABP after 6 months to test if reward-learning processes in the NAc are involved in the development of CBP. Additionally, we compared patients with CBP with controls to test the role of vmPFC-dependent reward-learning processes in the maintenance of chronic pain (see Table 1 for details on patients and controls). We used traditional univariate analysis methods to test if the development and maintenance are predicted by the magnitude of the learning-related responses in the NAc and vmPFC and learning-related connectivity between NAc and vmPFC. Additionally, we used multivariate pattern analyses (MVPA) to explore the role of learning-related response patterns. To test if any connectivity-based predictors are specific to the activations seen in the learning task, we additionally examined if resting state vmPFC-NAc connectivity mediates these predictions.

RESULTS

Reward learning and the transition to chronic pain: ROI and connectivity analysis

To test if the transition from SABP to CBP can be predicted by increased NAc responses to reward prediction errors, we extracted parameter estimates from pre-defined regions of interest (ROIs) of the bilateral NAc during reward feedback. Feedback without reward delivery was used to estimate negative prediction errors (NPE), and feedback with reward delivery was used to estimate positive prediction errors (PPEs). To test if chronicity was predicted by other aspects of instrumental learning than PPE/NPE or if this was a specific learning-related factor driving the development of chronic pain, we extracted parameter estimates from the NAc and vmPFC during the presentation of the discriminative stimuli, the anticipation of money and pain relief, and the painful stimulus. Further, we tested if changes of the vmPFC and NAc response to discriminative stimuli after the acquisition or extinction are underlying the transition from subacute to chronic pain by extracting the parameter estimates of both types of discriminative stimuli during habituation and extinction and calculated the contrast with the encoding of the same stimulus during acquisition. These parameter estimates were subsequently correlated with the percentage of change in pain severity from baseline to the follow-up assessment, and receiver operating characteristic (ROC) curves were created to dissociate patients with persistent SABP from recovered patients with SABP, based on a pain reduction of 20%.[8]

Higher blood-oxygen-level-dependent (BOLD) responses to monetary PPEs ($r(46) = 0.61$, $p < 0.001$) as well as in response to monetary NPEs ($r(46) = 0.55$, $p = 0.002$) in the left NAc indicated pain persistence. Binary classification analysis confirmed these results and showed a classification accuracy that was significantly higher than chance-level based on monetary PPE (area under the curve [AUC] = 0.77, $p = 0.021$) and monetary NPE (AUC = 0.83, $p < 0.001$) signals in the left NAc (see Figure 2). Contrary to our hypothesis, NAc responses to PPEs and NPEs for pain relief did not significantly predict chronicity (all $r(46) < 0.19$, $p = 1.00$, all AUC < 0.64, $p = 1.00$; see Table S4). Encoding of the discriminative stimuli (all $r(46) < 0.34$, $p > 0.82$, all AUC < 0.57, $p = 1.00$), the anticipation of reward (all $r(46) < 0.09$, $p = 1.00$, all AUC < 0.54, $p = 1.00$), or the painful stimulus (all $r < 0.37$, $p > 0.55$, and all AUC < 0.69, $p > 0.80$; for detailed information on correlation coefficients, AUC in binary classification, and significance values, see Table S4) also did not significantly predict chronicity. Further, the encoding of the discriminative stimuli during habituation (all $r(46) < 0.34$, $p > 0.55$, and all AUC < 0.72, $p > 0.15$) or extinction (all $r(46) < 0.17$, $p = 1.00$, and all AUC < 0.55, $p = 1.00$), as well as the change in neural representation of the discriminative stimuli from the habituation to the acquisition phase (all $r(46) < 0.26$, $p = 1.00$, and all AUC < 0.73, $p > 0.11$), or from the acquisition to the extinction phase (all $r(46) < 0.28$, $p = 1.00$, and all AUC < 0.56, $p = 1.00$; for detailed information on correlation coefficients, AUC in binary classification, and significance values, see Table S6) did not significantly predict chronicity.

In the next step, we tested if changes in functional connectivity between vmPFC and NAc during reward learning predicted pain persistence. We performed a psychophysiological interaction analysis on the reward-learning data of the patients with SABP with the vmPFC as a seed region. Pain persistence was predicted by higher functional connectivity between right NAc and vmPFC during monetary NPEs ($r(46) = 0.52$, $p = 0.006$). Binary classification of persistence by rNAc-vmPFC functional

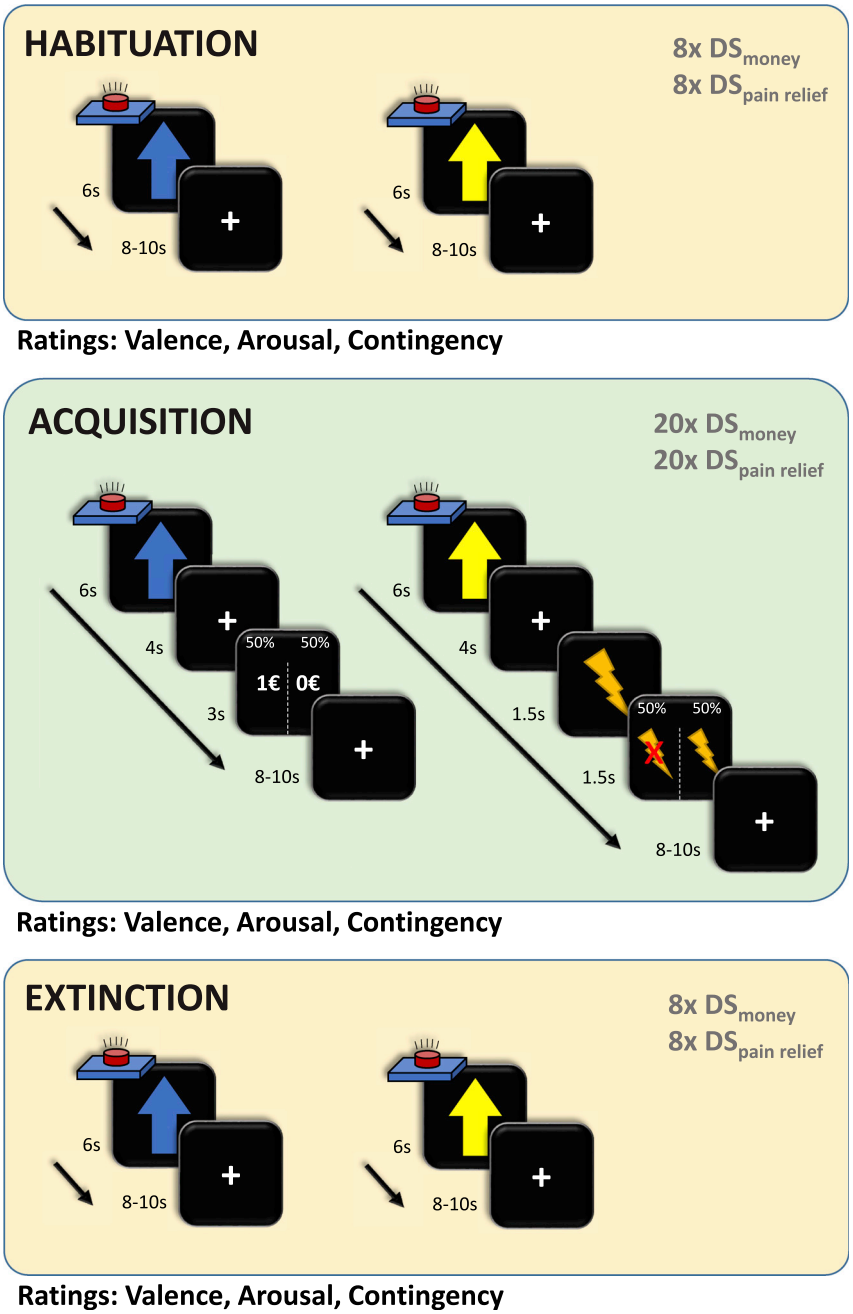

Figure 1. Study design

All participants underwent three phases of the experiment: habituation, acquisition, and extinction. During the habituation and extinction phases, both discriminative stimuli (DS_{pain} and DS_{money}, blue and yellow arrows on black background, respectively, duration: 6 s) were presented eight times each and followed by an inter-trial interval of 8–10 s (random jitter). During acquisition, twenty DS of each type were presented for 6 s and followed by an anticipation phase of 4 s. In the monetary reward condition, a monetary reward (1 €) or no reward (fixation cross) was subsequently presented for 3 s. In the pain-relief condition, the anticipation phase was always followed by a painful stimulus lasting 1.5 s. During the feedback phase of the pain-relief condition, participants received either pain relief (no pain) or pain (pain for 1.5 s). Participants were instructed to press a button with their index finger as soon as they saw any of the two discriminative stimuli, with the goal of winning a monetary reward or pain relief if they pressed the button "fast enough." In reality, both rewards were delivered in 50% of the trials. Participants never received rewards if they did not press the button. The feedback phase was followed by an inter-trial interval of 8–10 s (random jitter). Ratings of the contingency between each DS and the rewards (numerical rating scale from 1 to 9) and the arousal and valence associated with each DS (self-assessment manikins converted to a scale from 1 to 9) were presented after the habituation, acquisition, and extinction phases.

connectivity during monetary NPEs was also significantly higher than chance-level classification (AUC = 0.78, p = 0.021; see Figure 2). Neither alterations in functional connectivity between vmPFC and NAc during PPEs and NPEs for pain relief (all r(46) < 0.42, p > 0.19, and all AUC < 0.67, p = 1.00) nor during discriminative stimuli (all r(46) < 0.42, p > 0.16, and all AUC < 0.55, p = 1.00), anticipation (all r(46) < 0.21, p = 1.00, and all AUC < 0.65, p = 1.00), or the painful stimulus (all r(46) < 0.14, p = 1.00, and all AUC < 0.47, p = 1.00) significantly predicted the transition from subacute to chronic pain (see Table S5).

Resting-state prediction of the transition to chronic pain

Next, we tested if functional vmPFC-NAc connectivity per se, or specifically related to PPEs/NPEs, predicted chronicity. For this purpose, the functional connectivity between vmPFC and NAc was analyzed from a separate resting-state acquisition at baseline. We found that increased resting-state functional connectivity between vmPFC and left NAc (r(42) = 0.36, p = 0.035; AUC = 0.68, p = 0.043), but not right NAc (r(42) = 0.17, p = 0.53; AUC = 0.66, p = 0.071), significantly predicted pain persistence after 6 months (see Figure 3). We therefore tested if the encoding of PPEs/NPEs in the vmPFC-NAc pathway that was predictive for chronicity (see above) was mediated by resting-state connectivity between vmPFC and left/right NAc but found no significant mediation of the effect of task-based prediction error encoding on pain chronicity via resting-state vmPFC-NAc connectivity (indirect effect given as average causal mediation effects [ACMEs]: all ACME < 0.05, p > 0.36; see Figure S5). This suggests that the encoding of PPEs/NPEs in the vmPFC-NAc pathway and resting-state connectivity between vmPFC and lNAc independently

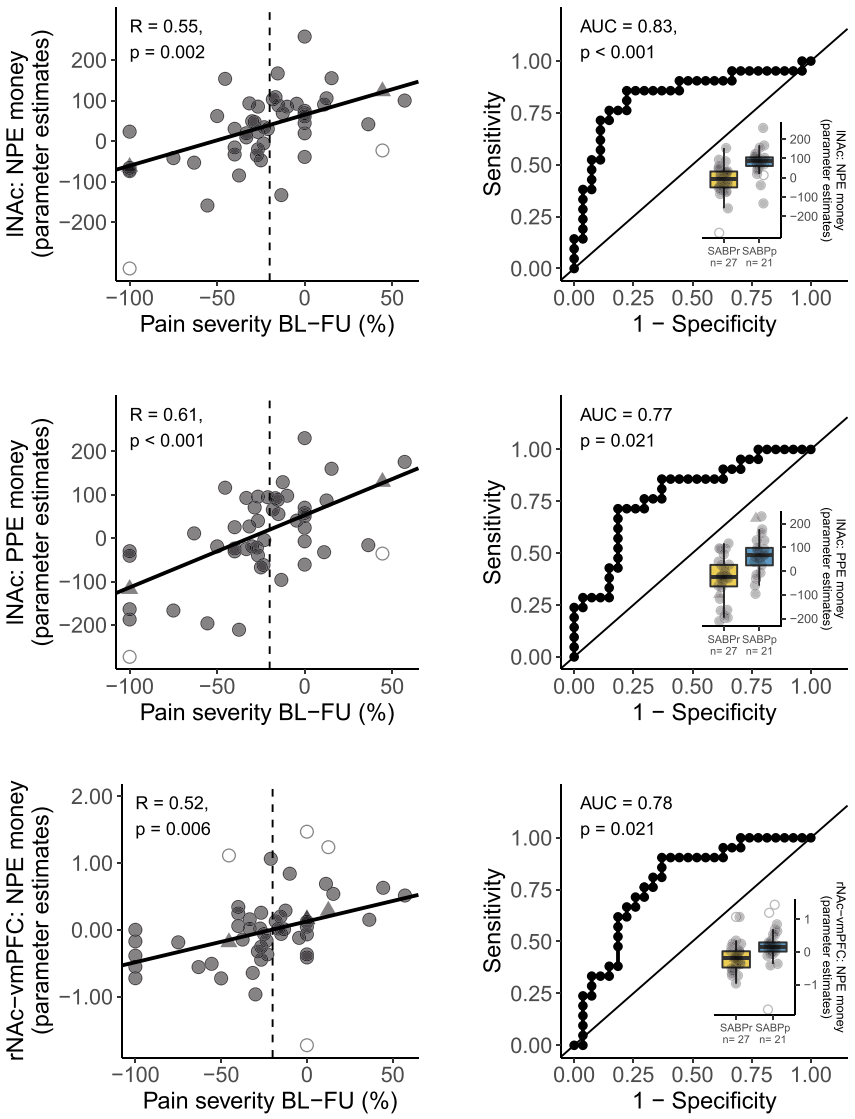

Figure 2. Fronto-striatal encoding of prediction error signal predicts the transition from subacute to chronic pain

(Left) Correlations of the percentage of change in pain severity from baseline to the 6 month follow up and the BOLD response to prediction errors in the NAc and vmPFC. The dashed vertical line indicates the 20% cutoff that was used to binarize the change in pain severity for the receiver operating characteristic (ROC) curves on the right side. BOLD responses were extracted as parameter estimates from predefined masks extracted from http://neurosynth.org (see STAR methods). Correlations are reported as Pearson's correlation with Bonferroni-corrected p values (corrected for 45 tests, yielding a threshold of $p < 0.001$). (Right) We additionally divided patients in "recovered" if their pain severity decreased by 20% or more between the first examination and the follow-up assessment and "persistent" patients in all other instances. ROC curves were created for classifying recovered and persistent patients with the respective parameter estimates extracted from the regions of interest. We report the area under each ROC curve as an estimate of sensitivity and specificity. Associated p values for the comparison to a chance-level ROC curve (i.e., AUC = 0.5) are reported as Bonferroni-corrected p values (corrected for 45 tests, yielding a threshold of $p < 0.001$). Boxplots additionally show the distribution of patients who recovered (yellow) and patients with persistent pain at follow up (blue). The hinges of the boxplots represent the first and third quartiles, and the whiskers extend to the last value within 1.5 times the interquartile range. Single data points are shown as circles. Outliers are depicted as empty circles and imputed values as triangles. See Tables S4 and S5 for all other associations between reward-learning contrasts and change in pain severity. vmPFC, ventromedial prefrontal cortex; lNAc, left nucleus accumbens; rNAc, right nucleus accumbens; PPE, positive prediction error; NPE, negative prediction error; BL, baseline; FU, follow up; AUC, area under the curve; SABP, patients with subacute back pain; SABPp/r, patients with SABP with persistent pain or recovered pain after 6 months, based on a pain reduction of 20% from baseline to the follow-up assessment.

predict chronicity. We therefore tested if adding resting-state connectivity between vmPFC and left NAc (and the interaction term with the respective task-based predictor) to the regression models would improve the model fit. Adding resting-state connectivity significantly improved the prediction of chronicity with the encoding of NPE_{money} in the left NAc (original model: adjusted $R^2 = 0.290$, new model: adjusted $R^2 = 0.364$, difference between models: $F(2,44) = 3.67$, $p = 0.033$) and the prediction of chronicity with functional connectivity between right NAc and vmPFC during NPE_{money} (original model: adjusted $R^2 = 0.259$, new model: adjusted $R^2 = 0.356$, difference between models: $F(2,44) = 4.46$, $p = 0.017$). Adding resting-state connectivity to the prediction of chronicity with the encoding of PPE_{money} in the left NAc did not significantly improve model fit (original model: adjusted $R^2 = 0.353$, new model: adjusted $R^2 = 0.409$, difference between models: $F(2,44) = 3.17$, $p = 0.052$).

Reward learning and the transition to chronic pain: Pattern decoding

We additionally performed an exploratory analysis to test if specific patterns in the vmPFC and bilateral NAc as well as patterns of functional connectivity between vmPFC and NAc predict chronicity. We used the same regressors as for the univariate analysis and trained a linear discriminant analysis (LDA) classifier and extracted the mean classification accuracy across folds for each subject and found a pattern of activity in response to the discriminative stimulus for pain relief in the right NAc, which classified patients into patients with persistent SABP and recovered patients, with an accuracy of 71% ($t(47) = 4.30$, $p = 0.004$; AUC = 0.80, $p = 0.009$; see Figure 4). No other brain responses yielded

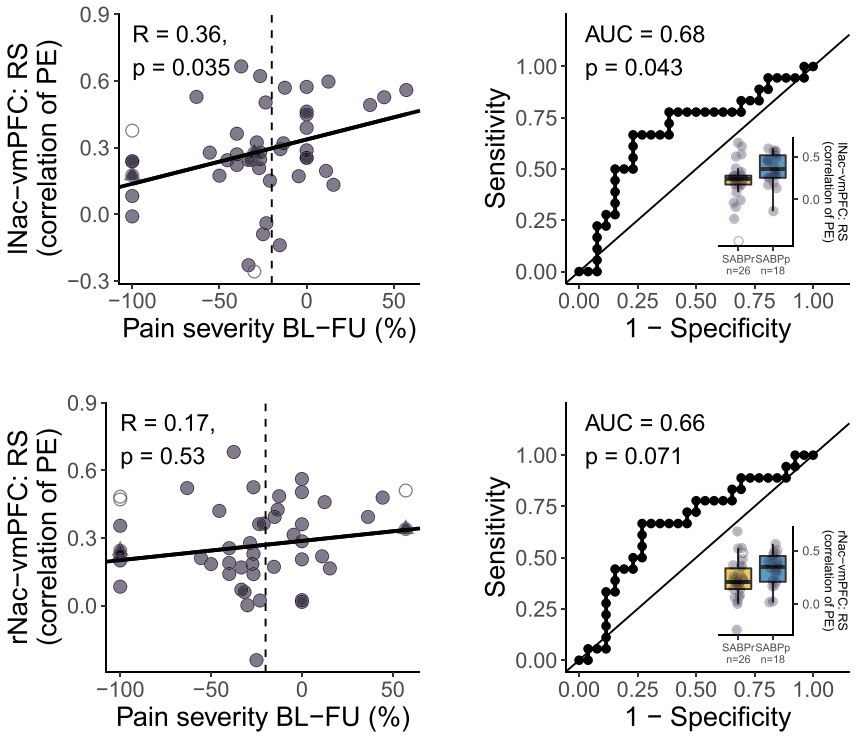

Figure 3. Functional connectivity of NAc and vmPFC independent of learning (i.e., resting-state functional connectivity) shows low predictive value of the transition from subacute to chronic pain

(Left) Correlations of the percentage of change in pain severity from baseline to the 6 month follow up with the resting-state functional connectivity between vmPFC and bilateral NAc. The dashed vertical line indicates the 20% cutoff that was used to binarize the change in pain severity for the ROC curves on the right side. Resting-state functional connectivity was extracted as the correlation between individual time series in predefined masks, which were extracted from http://neurosynth.org (see STAR methods). Correlations are reported as Pearson's correlation with Bonferroni-corrected p values (corrected for 2 tests, yielding a threshold of $p < 0.025$). (Right) Corresponding ROC curves were created for classifying recovered and persistent pain patients with the functional connectivity between vmPFC and NAc at rest. We report the area under each ROC curve as an estimate of sensitivity and specificity. Associated p values for the comparison to a chance-level ROC curve (i.e., AUC = 0.5) are reported as Bonferroni-corrected p values (corrected for 2 tests yielding an uncorrected threshold of $p < 0.025$). Boxplots additionally show the distribution of recovered patients (yellow) and patients with persistent pain at follow up (blue). The hinges of the boxplots represent the first and third quartiles, and the whiskers extend to the last value within 1.5 times the interquartile range. Single data points are shown as circles. Outliers are depicted as empty circles and imputed values as triangles. vmPFC, ventromedial prefrontal cortex; lNAc, left nucleus accumbens; rNAc, right nucleus accumbens; BL, baseline; FU, follow up; AUC, area under the curve; RS, resting state; PE, parameter estimates; SABP, patients with subacute back pain; SABPp/r: patients with SABP with persistent pain or recovered pain after 6 months, based on a pain reduction of 20% from baseline to the follow-up assessment.

any pattern of activity (all $t(47) < 2.49$, $p > 0.74$; all AUC <0.69, $p > 0.84$; see Table S7) or connectivity (all $t < 3.17$, $p > 0.12$; all AUC < 0.74, $p > 0.10$; see Table S8) that significantly classified patients into recovered and persistent patients above chance level.

An additional whole-brain searchlight MVPA analysis did not yield any significant predictions related to activations in other brain regions for the transition from subacute to chronic pain following appropriate multiple comparisons corrections.

Reward-learning characteristics in chronic pain: ROI and connectivity analysis

To check whether the vmPFC response during reward anticipation and discriminative signals is characteristic for the chronic stage of back pain, we employed the same reward-learning paradigm that we used for patients with SABP and compared patients with CBP with controls. In patients with CBP, we found significantly lower BOLD responses in the vmPFC compared with controls during PPEs for monetary reward (cluster size = 7 voxels, coordinates [MNI] of peak voxel: x = −4.5, y = 49.5, z = −2.5, p(FWE) = 0.04, t(max) = 3.48) and significantly higher BOLD responses in the vmPFC in response to a discriminative stimulus for monetary reward (cluster size = 48 voxels, coordinates [MNI] of peak voxel: x = −0.5, y = 55.5, z = −8.5, p(FWE) = 0.01, t(max) = 3.69). A very small cluster of voxels in the left NAc further showed significantly higher functional connectivity with the vmPFC in patients with CBP compared with controls during PPEs for monetary reward (cluster size = 2 voxels, coordinates [MNI] of peak voxel: x = −12.5, y = 9.5, z = −10.5, p(FWE) = 0.03, t(max) = 4.2; see Figure 5). Neither activity in NAc, nor in vmPFC, nor functional connectivity between vmPFC and NAc significantly differed between patients with CBP and controls during any other reward-learning process.

To test if reward learning was associated with pain severity in patients with CBP, we extracted parameter estimates from predefined ROIs of the vmPFC and bilateral NAc for each contrast and each individual. We then correlated ongoing pain severity with those parameter estimates. Encoding of PPEs and NPEs (all $r(27) < 0.36$, $p = 1.00$, and all AUC < 0.56, $p = 1.00$), discriminative stimuli (all $r(27) < 0.35$, $p = 1.00$, and all AUC < 0.63, $p = 1.00$), the anticipation of reward (all $r(27) < 0.37$, $p = 1.00$, and all AUC < 0.60, $p = 1.00$), or the painful stimulus (all $r(27) < 0.10$, $p = 1.00$, and all AUC < 0.59, $p = 1.00$) was not significantly correlated to back-pain severity in patients with CBP (see Figure 5 and Table S9). Also, functional connectivity between vmPFC and NAc during PPEs and NPEs (all $r(27) < 0.28$, $p = 1.00$, and all AUC < 0.62, $p = 1.00$), discriminative stimuli (all $r(27) < 0.23$, $p = 1.00$, and all AUC < 0.64, $p = 1.00$), anticipation (all $r(27) < 0.36$, $p = 1.00$, and all AUC < 0.56, $p = 1.00$), or the painful stimulus (all $r(27) < 0.38$, $p = 1.00$, and all AUC < 0.54,

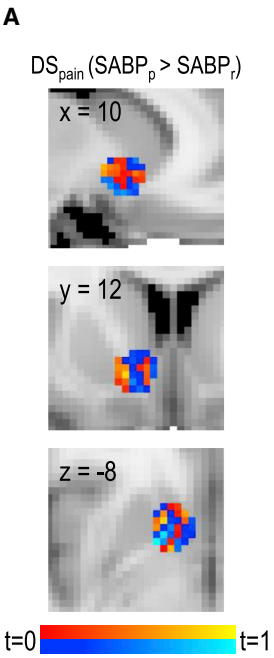

Figure 4. Pattern of responses to the discriminative stimulus for pain relief in the right NAc predicts transition from subacute to chronic pain

(A) Patterns of voxelwise t scores from the contrast DS$_{pain}$ (SABP$_p$ > SABP$_r$). Warm colors depict voxels with higher responses in patients with persistent pain, while cool colors depict voxels with higher responses in recovered patients.

(B) The corresponding ROC curve for classifying recovered and persistent-pain patients based on the multivariate classifiers. We report the area under the ROC curve as an estimate of sensitivity and specificity. Associated p values for the comparison to a chance-level ROC curve (i.e., AUC = 0.5) are reported as Bonferroni-corrected p values (corrected for 45 tests, yielding a threshold of $p < 0.001$). The boxplot additionally shows the probability of being classified as a patient with persistent pain for recovered patients (yellow) and patients with persistent pain at follow up (blue). The hinges of the boxplots represent the first and third quartiles, and the whiskers extend to the last value within 1.5 times the interquartile range. Single data points are shown as black circles. rNAc, right nucleus accumbens; DS, discriminative stimulus; AUC, area under the curve; SABP, patients with subacute back pain; SABPp/r: patients with SABP with persistent pain or recovered pain after 6 months, based on a pain reduction of 20% from baseline to the follow-up assessment.

p = 1.00) was not significantly correlated with pain severity in patients with CBP (see Figure 5 and Table S10).

Resting-state characteristics of chronic pain

We further tested if increased functional vmPFC-NAc connectivity per se, or specifically related to PPE/NPE, characterized chronicity. For this purpose, we analyzed the functional connectivity between vmPFC and NAc based on an initial MR session but found no difference between patients with CBP and controls in functional resting-state connectivity between vmPFC and left (AUC = 0.42, p = 1.00) or right NAc (AUC = 0.47, p = 1.00; see Figure 6).

DISCUSSION

This study investigated to what extent the encoding of operant-learning processes in the vmPFC-NAc pathway can be utilized to predict the development of CBP and to what extent it characterizes the chronic stage of back pain. In patients with SABP, the transition to chronic pain was best predicted by increased monetary reward prediction error signals in the NAc as well as an increase in functional connectivity between the vmPFC and the NAc related to NPEs. In patients with CBP, compared with controls, we found a reduced vmPFC response during encoding of positive monetary reward prediction errors but an increased vmPFC response to a discriminative stimulus of monetary rewards. Resting-state vmPFC-NAc connectivity predicted chronicity independent of task-based prediction of chronicity but was not characteristic for the chronic stage of back pain. This supports the view of learning-related adaptations in the vmPFC-NAc pathway during the transition to chronic pain[28] and also indicates a role of the vmPFC-NAc pathway in the transition to chronic pain that is independent of operant learning.

Reward prediction error signals serve as a teaching signal in reinforcement learning to promote behavior that will maximize future rewards.[29] Together, the vmPFC and NAc represent a fronto-striatal loop that is essential in coding rewarding events.[30] Reward prediction errors are encoded by phasic dopamine signaling in the NAc,[14,31] while dopamine-dependent activity in the vmPFC tracks the learned value of signals to evaluate the likelihood of obtaining the reward after a given behavior.[32] Baliki et al. showed evidence of the predictive value of the vmPFC-NAc pathway for the development of chronic pain.[8] Our current data confirm and extend these findings, suggesting that patients who later develop chronic pain have a hyperactive reward updating system during the subacute phase of their pain. This is in line with the finding that food reward enhances dopamine levels in the NAc in early stages of a rat SNL model but not in later stages.[19] Furthermore, negative reinforcement (analgesic treatment with clonidine) in a similar time window after SNL promotes conditioned place preference, mediated by enhanced dopamine levels in the NAc.[33] The same effect of negative reinforcement (analgesic treatment via peripheral nerve block) on conditioned place preference and increased dopamine levels in the NAc was reported in a very early time window (24 h) but not 96 h after incision injury in rats but was blocked after the injection of the selective dopamine antagonist flupenthixol into the NAc.[16] In light of these findings and the data presented in the current study, the vmPFC-NAc response to pain variations found by Baliki et al.[8] might have been related to an updating process of signals

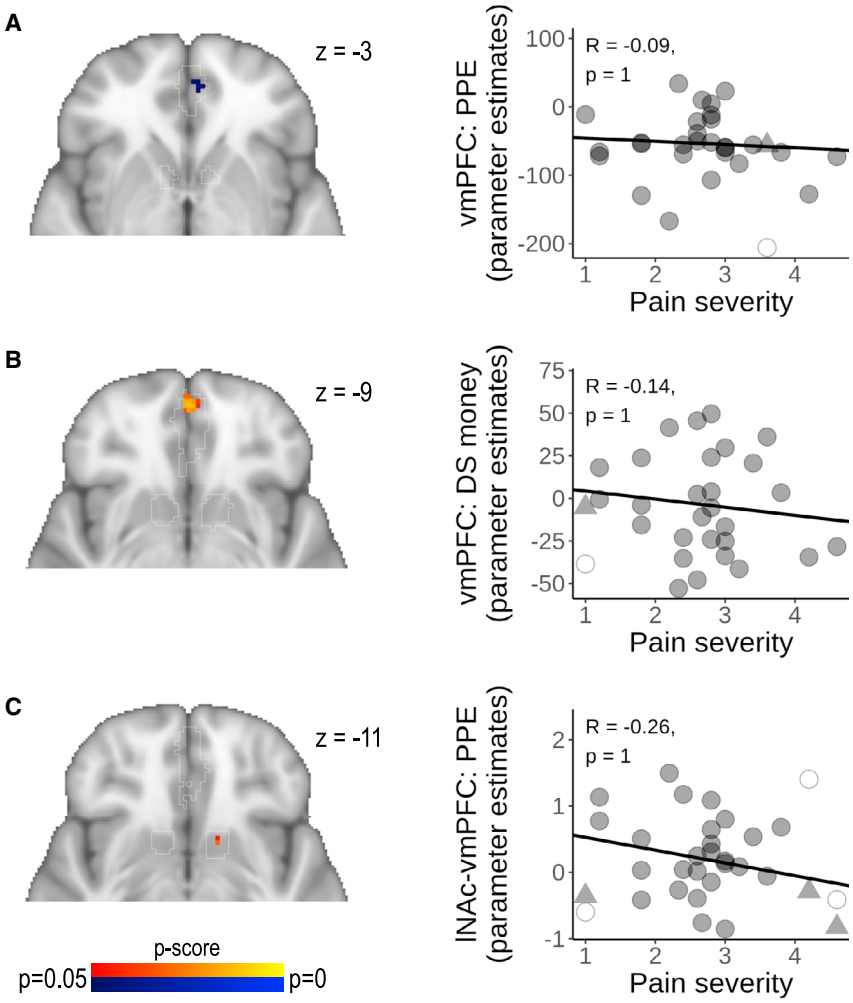

Figure 5. Patients with CBP are characterized by reduced vmPFC responses to prediction error and increased responses to a discriminative stimulus

(A–C) (Left) BOLD responses to (A) positive monetary reward prediction error, (B) the discriminative stimulus for monetary rewards, and (C) functional connectivity between left NAc and vmPFC during positive monetary reward prediction error are depicted as p maps and were calculated using non-parametric two-sample t tests (CBP > HC shown in red and yellow, CBP < HC shown in blue and light blue) within a mask of vmPFC and NAc, with bootstrapping, using 5,000 permutations (all reward-learning contrasts that dissociated HC and CBP in vmPFC and NAc are shown).

(Right) No significant correlations were found between pain severity in patients with CBP and the BOLD response in predefined masks of the vmPFC and NAc for the respective contrast. Outliers are depicted as empty circles and imputed values as triangles. See Tables S9 and S10 for all other associations between reward-learning contrasts and pain severity. vmPFC, ventromedial prefrontal cortex; lNAc, left nucleus accumbens; DS, discriminative stimulus; PPE, positive prediction error for monetary rewards.

for the negative reinforcement experienced during phases of pain relief, which is in line with the idea that NAc activity predicts reward (pain relief) magnitude at stimulus offset.[34]

Interestingly, in our study, we showed a hyperactive reward updating system only for monetary rewards but not for pain relief as a reward. This is contrary to the finding by Kato et al.,[19] who observed enhanced dopamine levels in the NAc in response to pain relief in an early, but not in a later, time window after SNL. This could have different reasons: first, the NAc response to pain relief is enhanced in early time windows but has no effect on the subsequent development of chronic pain. Second, the feedback phase in our pain-relief condition was 50% shorter than in the monetary reward condition, therefore lowering the statistical power of the prediction error signal in this condition. Indeed, increased connectivity between vmPFC and rNAc during the encoding of NPEs for pain relief showed a small, but non-significant, correlation ($r = 0.41$, $p = 0.19$; binary classification: AUC = 0.66, $p = 1.00$). Third, in the current study, we used relief from evoked pain as a negative reinforcement. In such cases, the signal for pain relief cannot be as clearly dissociated from the signal for pain, as in the case of ongoing pain.[35] It is therefore possible that we rather showed that updating a punishing pain signal was not predictive of pain chronicity than showing the same for a signal of pain relief.

Of note, vmPFC-NAc connectivity at rest predicted chronicity independent of learning-related responses in the vmPFC-NAc pathway. This extends findings from a spared nerve injury (SNI) model of chronic pain showing no altered fronto-striatal resting-state connectivity but decreased connectivity of the NAc to the insular, primary, and secondary sensory cortices, caudate, and putamen.[36] Importantly, these pathways were not tested in the current study, and the differences between sham and SNI treated rats were found 28 days after surgery and therefore represent alterations at the chronic stage and not necessarily predictive mechanisms. The absence of alterations in vmPFC-NAc connectivity at rest is therefore in line with our negative finding in patients with CBP compared with controls and a recent study in humans showing decreased functional integration of the vmPFC at rest, evidenced by lower global efficiency, degree, and betweenness centrality in patients with CBP compared with controls.[24]

Chronicity was further predicted by a pattern of activity in response to a signal that contains previously acquired information on the probability of pain/pain relief (discriminative stimulus) but not by reward prediction error signals. Pattern analyses are not sensitive to response magnitude in a cluster of voxels but rather to the relative pattern of activity in different voxels within this cluster. The absence of predictive value of reward prediction

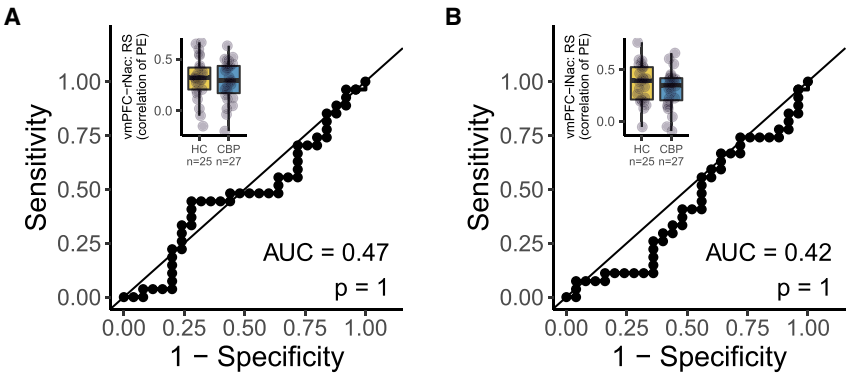

Figure 6. Functional connectivity of NAc and vmPFC at rest does not dissociate patients with chronic back pain and controls

(A and B) ROC curves were created for classifying patients with chronic back pain and controls based on the functional connectivity between vmPFC and (A) right NAc and (B) left NAc, respectively. We report the area under each ROC curve as an estimate of sensitivity and specificity. Associated p values for the comparison to a chance-level ROC curve (i.e., AUC = 0.5) are reported as Bonferroni-corrected p values (corrected for 2 tests, yielding an uncorrected threshold of $p < 0.025$). Boxplots additionally show the distribution of patients with CBP (yellow) and controls (blue). The hinges of the boxplots represent the first and third quartiles, and the whiskers extend to the last value within 1.5 times the interquartile range. Single data points are shown as circles. vmPFC, ventromedial prefrontal cortex; lNAc, left nucleus accumbens; rNAc, right nucleus accumbens; BL, baseline; FU, follow up; AUC, area under the curve; RS, resting state; PE, parameter estimates.

error patterns therefore does not contradict our results from the univariate analysis but rather shows additional reorganization within the NAc. The spatial distribution of this pattern does not seem to represent a functional distinction of NAc core and shell (see Figure 4), which was previously discussed to encode expectancy of monetary reward and pain relief.[37] Rather, distinct subgroups of neurons in the NAc respond to different functions during reward learning, such as cue responses, motor-response initiation, or the encoding of different reward intensities.[38] Future studies should therefore investigate spatial reorganization of cue-responsive neurons in the NAc, as these may characterize patients at risk for developing chronic pain.

We further found that, compared with controls, patients with CBP showed increased vmPFC responses to the discriminative stimulus of the monetary reward condition, while the monetary reward prediction error signal in the vmPFC was decreased. Therefore, patients with CBP showed increased vmPFC responses to a signal that contained previously acquired information on reward probability but reduced activation to a signal containing new information on stimulus-reward contingencies. This is in line with a previous study in patients with CBP, which reported that impaired explorative behavior was associated with a loss of distinction between positive and negative feedback in the P300 component and an inverted feedback-related negativity recorded at frontal electrodes (Fz) in the electroencephalogram (EEG),[26] two evoked potentials that were previously connected to reward prediction error processing.[39]

Our results indicate that in the chronic stage of back pain, the evaluation of an established reward signal is enhanced at the cost of an updating of this signal to better adapt to a changing environment, or, in other words, patients with CBP show impaired vmPFC responses during learning from reward but increased sensitivity to reward signals. This is in line with the finding that patients with chronic pain are less responsive to rewards, while the drive to receive rewards is not decreased.[40] On the neurochemical level, this may be related to (tonic) hypodopaminergic states in chronic pain. Such a hypodopaminergic state has been shown in patients with fibromyalgia, who showed reduced L-Dopa uptake in the ventral tegmental area, thalamus, hippocampus, anterior cingulate cortex, and the insular cortex,[41] in patients with CBP, who showed reduced D2/D3 receptor binding in the ventral striatum,[42] and in patients with burning mouth syndrome, who showed reduced striatal D1 receptor binding.[43] While phasic dopamine activity in the NAc drives a reevaluation of existing stimulus-reward contingencies, tonic dopamine release modulates the responsiveness of NAc neurons to inputs from medial prefrontal cortex.[44]

In summary, the way neural pathways respond to the exploration-exploitation dilemma in reward learning predicts the development of chronic pain and characterizes the chronic stage of back pain. While the vmPFC-NAc pathway is highly sensitive during the exploration of potential reward signals during the transition from subacute to chronic pain, the same pathway is more sensitive during the exploitation of past stimulus-reward associations in patients with chronic pain, even if these contingencies may no longer be appropriate. Increasing the variability of behavioral responses and fostering explorative behavior may be a valuable treatment target in patients with chronic pain.[45] Behavioral treatments targeting operant-learning mechanisms are available,[46,47] and Ashar et al.[48] showed that brain connectivity patterns may predict successful cognitive-behavioral treatment of CBP. Moreover, the transition from subacute to CBP was prevented in patients treated with Levodopa combined with naproxen and was associated with a normalization of altered vmPFC-NAc connectivity specifically in female patients with SABP, while naproxen alone did not have beneficial effects.[49]

Therefore, treatment and prevention of CBP could be improved by allocating patients to dopaminergic treatments, operant therapies, or their combination based on behavioral and vmPFC-NAc responses during reward learning. Identification of risk groups may further be improved by studying the association of fronto-striatal reward processing with genetic risk factors.[50]

Limitations of the study

The present data need to be considered in the light of several limitations. First, the aforementioned methodological considerations do not allow final conclusions on the predictive role of vmPFC-NAc processing of pain relief. Second, our follow-up assessment in patients with SABP was carried out after

Table 1. Patient characteristics: All values show the mean and standard deviation for each individual group

	SABP	SABPp	SABPr	CBP	HC	Missings
N	48	21	27	29	29	NA
Age	35.0 (13.4)	36.6 (13.9)	33.8 (13.0)	38.7 (15.8)	35.7 (14.7)	0/0/0/0/0
Gender (m/f)	18/30	6/15	12/15	16/13	17/12	0/0/0/0/0
Number of days with pain during last year	66.2 (42.9)	57.6 (32.6)	73.0 (49.1)	241 (92.3)	NA	7/3/4/2/NA
Time since first pain episode (months)[a]	25.2 [4.3, 119.9]	28.5 [4.4, 100.6]	21.8 [6.1, 119.9]	62.5 [18.8–145.3]	NA	0/0/0/0/NA
Delta pain severity (FU-BL): absolute	−0.91 (1.19)	0.05 (0.69)	−1.65 (0.93)	NA	NA	0/0/0/NA/NA
Delta pain severity (FU-BL): percentage	−25.7 (35.9)	3.4 (20.4)	−48.3 (28.1)	NA	NA	0/0/0/NA/NA
Pain severity (MPI)	2.33 (0.93)	2.42 (0.92)	2.27 (0.95)	2.67 (0.85)	NA	0/0/0/1/NA
Interference (MPI)	1.81 (1.11)	2.05 (1.17)	1.63 (1.04)	2.47 (1.10)	NA	4/2/2/4/NA
Negative mood (MPI)	2.67 (1.18)	2.75 (1.16)	2.61 (1.21)	2.71 (1.03)	NA	4/2/2/4/NA
Life control (MPI)	3.92 (1.27)	3.88 (1.28)	3.96 (1.28)	3.92 (1.02)	NA	4/2/2/4/NA
Support (MPI)	2.17 (1.82)	2.39 (1.92)	2.00 (1.76)	2.72 (1.67)	NA	6/3/3/4/NA
CPG[a]	1.00 [0, 2]	2.00 [0, 2]	1.00 [0, 2]	2.00 [0.5, 3.00]	NA	6/4/2/6/NA
ÖMPQ	72.0 (31.1)	71.9 (34.1)	72.1 (29.2)	82.2 (35.9)	NA	0/0/0/1/NA
Anxiety (HADS)	7.23 (3.98)	7.06 (3.93)	7.36 (4.09)	7.32 (4.50)	3.54 (2.39)	5/3/2/4/3
Depression (HADS)	4.81 (4.01)	4.33 (2.83)	5.16 (4.71)	5.59 (4.08)	2.96 (4.24)	5/3/2/4/3
Perceived stress (PSS)	18.1 (6.84)	18.1 (7.19)	18.0 (6.70)	17.9 (7.63)	9.88 (5.76)	4/2/2/4/5

MPI, West Haven-Yale Multidimensional Pain Inventory; CPG, Chronic Pain Grade; ÖMPQ, Örebro Musculoskeletal Pain Questionnaire; HADS, Hospital Anxiety and Depression Scale; HC, healthy control; CBP, chronic back pain; SABP, patients with subacute back pain; SABPp/r, patients with SABP with persistent pain or recovered pain after 6 months, based on a pain reduction of 20% from baseline to the follow-up assessment; FU, follow up after 6 months; BL, baseline assessment; SD, standard deviation.

[a]For the Chronic Pain Grade and pain onset, the median and interquartile range are depicted.

6 months. Previous research found gray-matter density changes in the NAc after only 12 months and predicted pain severity on the basis of functional connectivity between the vmPFC and NAc after 12 months but not after 7 weeks or 6 months.[8] Future studies will have to investigate if the predictive value of enhanced updating processes in the vmPFC-NAc pathway is stable also in later stages of chronicity. Third, we focused our hypotheses and analyses on the role of the vmPFC-NAc pathway. This pathway is not independent of other areas such as the dorsal parts of the PFC, the ventral tegmental area (VTA), anterior cingulate cortex (ACC), putamen, and caudate, which are involved in critical aspects of reward learning[27,51–55] and need to be investigated for their relevance to pain chronicity. Fourth, our limited sample size precluded the consideration of several potential moderating effects beyond brain functions such as peripheral, psychological, and social factors. We would therefore like to emphasize that additional variables not covered in this analysis may be important contributors to pain chronicity in addition to the neural response of the vmPFC-NAc pathway during reward learning. Fifth, the results related to altered prediction error encoding in patients with CBP compared with controls show only very small clusters of reduced BOLD responses in the vmPFC and increased vmPFC-NAc connectivity, and the predictive effect of vmPFC-NAc connectivity at rest is small. These effects therefore require replication to estimate their robustness. Future studies should aim for higher sample sizes to confirm our results

and to investigate the effects of moderating factors. Sixth, especially, our negative findings on neural response patterns have to be viewed in light of the limited spatial resolution of our functional images (2.3 × 2.3 × 3 mm).

STAR★METHODS

Detailed methods are provided in the online version of this paper and include the following:

- KEY RESOURCES TABLE
- RESOURCE AVAILABILITY
  - Lead contact
  - Materials availability
  - Data and code availability
- EXPERIMENTAL MODEL AND SUBJECT DETAILS
  - Subjects
  - Clinical assessments
- METHOD DETAILS
  - Experimental procedures
  - Magnetic resonance imaging
  - Regions of interest
- QUANTIFICATION AND STATISTICAL ANALYSIS
  - Preprocessing of magnetic resonance imaging data
  - Anatomical data preprocessing
  - Functional data preprocessing
  - Outlier detection, imputation, and correction for multiple comparisons
  - Reward learning and the transition to chronic pain: ROI and connectivity analysis
  - Resting-state prediction of the transition to chronic pain
  - Reward learning and the transition to chronic pain: Pattern decoding
  - Reward learning characteristics in chronic back pain
- ADDITIONAL RESOURCES

SUPPLEMENTAL INFORMATION

Supplemental information can be found online at https://doi.org/10.1016/j.xcrm.2022.100677.

ACKNOWLEDGMENTS

This work was supported by a grant from the Deutsche Forschungsgemeinschaft (SFB1158/B03 to F.N. and H.F.).

AUTHOR CONTRIBUTIONS

Study concept and design, H.F., K.U., F.N., and M.L.; acquisition of data, M.L., K.U., and M.K.; analysis and interpretation of data, M.L., S.M.L., F.N., S.D., and H.F.; drafting of the manuscript, M.L., S.M.L., K.U., S.D., M.K., F.N., and H.F.; critical revision of the manuscript for important intellectual content, M.L., S.M.L., K.U., S.D., M.K., F.N., and H.F.; obtained funding, H.F. and F.N.; administrative, technical, or material support, M.L., S.M.L., and S.D.; study supervision, H.F. and F.N.

DECLARATION OF INTERESTS

The authors declare no competing interests.

Received: December 13, 2021
Revised: April 8, 2022
Accepted: June 13, 2022
Published: July 6, 2022

REFERENCES

1. Vlaeyen, J.W. (2015). Learning to predict and control harmful events: chronic pain and conditioning. Pain *156*, S86–S93. https://doi.org/10.1097/j.pain.0000000000000107.
2. Main, C.J., Keefe, F.J., Jensen, M.P., Vlaeyen, J.W., Vowles, K.E., and Fordyce, W.E. (2014). Fordyce's Behavioral Methods for Chronic Pain and Illness: Republished with Invited Commentaries (Wolters Kluwer, IASP Press).
3. Fordyce, W.E. (1976). Behavioral Methods for Chronic Pain and Illness (C.V. Mosby).
4. Flor, H., Knost, B., and Birbaumer, N. (2002). The role of operant conditioning in chronic pain: an experimental investigation. Pain *95*, 111–118. https://doi.org/10.1016/s0304-3959(01)00385-2.
5. Raichle, K.A., Romano, J.M., and Jensen, M.P. (2011). Partner responses to patient pain and well behaviors and their relationship to patient pain behavior, functioning, and depression. Pain *152*, 82–88. https://doi.org/10.1016/j.pain.2010.09.015.
6. Nees, F., Ditzen, B., and Flor, H. (in press). When shared pain is not half the pain: enhanced central nervous system processing and verbal reports of pain in the presence of a solicitous spouse. Pain.
7. Fordyce, W.E., Brockway, J.A., Bergman, J.A., and Spengler, D. (1986). Acute back pain: a control-group comparison of behavioral vs traditional management methods. J. Behav. Med. *9*, 127–140. https://doi.org/10.1007/bf00848473.
8. Baliki, M.N., Petre, B., Torbey, S., Herrmann, K.M., Huang, L., Schnitzer, T.J., Fields, H.L., and Apkarian, A.V. (2012). Corticostriatal functional connectivity predicts transition to chronic back pain. Nat. Neurosci. *15*, 1117–1119. https://doi.org/10.1038/nn.3153.
9. Leknes, S., Lee, M., Berna, C., Andersson, J., and Tracey, I. (2011). Relief as a reward: hedonic and neural responses to safety from pain. PLoS One *6*, e17870. https://doi.org/10.1371/journal.pone.0017870.
10. Seymour, B., Daw, N.D., Roiser, J.P., Dayan, P., and Dolan, R. (2012). Serotonin selectively modulates reward value in human decision-making. J. Neurosci. *32*, 5833–5842. https://doi.org/10.1523/JNEUROSCI.0053-12.2012.
11. Abler, B., Walter, H., Erk, S., Kammerer, H., and Spitzer, M. (2006). Prediction error as a linear function of reward probability is coded in human nucleus accumbens. Neuroimage *31*, 790–795. https://doi.org/10.1016/j.neuroimage.2006.01.001.
12. Pagnoni, G., Zink, C.F., Montague, P.R., and Berns, G.S. (2002). Activity in human ventral striatum locked to errors of reward prediction. Nat. Neurosci. *5*, 97–98. https://doi.org/10.1038/nn802.
13. Nicola, S.M., Yun, I.A., Wakabayashi, K.T., and Fields, H.L. (2004). Firing of nucleus accumbens neurons during the consummatory phase of a discriminative stimulus task depends on previous reward predictive cues. J. Neurophysiol. *91*, 1866–1882. https://doi.org/10.1152/jn.00658.2003.
14. Hart, A.S., Rutledge, R.B., Glimcher, P.W., and Phillips, P.E.M. (2014). Phasic dopamine release in the rat nucleus accumbens symmetrically encodes a reward prediction error term. J. Neurosci. *34*, 698–704. https://doi.org/10.1523/jneurosci.2489-13.2014.
15. Schultz, W. (2017). Reward prediction error. Curr. Biol. *27*, R369–R371. https://doi.org/10.1016/j.cub.2017.02.064.
16. Navratilova, E., Xie, J.Y., Okun, A., Qu, C., Eyde, N., Ci, S., Ossipov, M.H., King, T., Fields, H.L., and Porreca, F. (2012). Pain relief produces negative reinforcement through activation of mesolimbic reward–valuation circuitry. Proc. Natl. Acad. Sci. U S A *109*, 20709–20713. https://doi.org/10.1073/pnas.1214605109.

17. Wunderlich, K., Rangel, A., and O'Doherty, J.P. (2010). Economic choices can be made using only stimulus values. Proc. Natl. Acad. Sci. U S A *107*, 15005–15010. https://doi.org/10.1073/pnas.1002258107.

18. Kim, H., Shimojo, S., and O'Doherty, J.P. (2011). Overlapping responses for the expectation of juice and money rewards in human ventromedial prefrontal cortex. Cerebr. Cortex *21*, 769–776. https://doi.org/10.1093/cercor/bhq145.

19. Kato, T., Ide, S., and Minami, M. (2016). Pain relief induces dopamine release in the rat nucleus accumbens during the early but not late phase of neuropathic pain. Neurosci. Lett. *629*, 73–78. https://doi.org/10.1016/j.neulet.2016.06.060.

20. Apkarian, A.V. (2008). Pain perception in relation to emotional learning. Curr. Opin. Neurobiol. *18*, 464–468. https://doi.org/10.1016/j.conb.2008.09.012.

21. Vachon-Presseau, E., Tétreault, P., Petre, B., Huang, L., Berger, S.E., Torbey, S., Baria, A.T., Mansour, A.R., Hashmi, J.A., Griffith, J.W., et al. (2016). Corticolimbic anatomical characteristics predetermine risk for chronic pain. Brain *139*, 1958–1970. https://doi.org/10.1093/brain/aww100.

22. Fritz, H.C., McAuley, J.H., Wittfeld, K., Hegenscheid, K., Schmidt, C.O., Langner, S., and Lotze, M. (2016). Chronic back pain is associated with decreased prefrontal and anterior insular gray matter: results from a population-based cohort study. J. Pain *17*, 111–118. https://doi.org/10.1016/j.jpain.2015.10.003.

23. Makary, M.M., Polosecki, P., Cecchi, G.A., DeAraujo, I.E., Barron, D.S., Constable, T.R., Whang, P.G., Thomas, D.A., Mowafi, H., Small, D.M., and Geha, P. (2020). Loss of nucleus accumbens low-frequency fluctuations is a signature of chronic pain. Proc. Natl. Acad. Sci. U S A *117*, 10015–10023. https://doi.org/10.1073/pnas.1918682117.

24. Letzen, J.E., Boissoneault, J., Sevel, L.S., and Robinson, M.E. (2020). Altered mesocorticolimbic functional connectivity in chronic low back pain patients at rest and following sad mood induction. Brain Imaging Behav. *14*, 1118–1129. https://doi.org/10.1007/s11682-019-00076-w.

25. Berger, S.E., Baria, A.T., Baliki, M.N., Mansour, A., Herrmann, K.M., Torbey, S., Huang, L., Parks, E.L., Schnizter, T.J., and Apkarian, A.V. (2014). Risky monetary behavior in chronic back pain is associated with altered modular connectivity of the nucleus accumbens. BMC Res. Notes *7*, 1–14. https://doi.org/10.1186/1756-0500-7-739.

26. Tamburin, S., Maier, A., Schiff, S., Lauriola, M.F., Di Rosa, E., Zanette, G., and Mapelli, D. (2014). Cognition and emotional decision-making in chronic low back pain: an ERPs study during Iowa gambling task. Front. Psychol. *5*, 1350. https://doi.org/10.3389/fpsyg.2014.01350.

27. Martucci, K.T., Borg, N., MacNiven, K.H., Knutson, B., and Mackey, S.C. (2018). Altered prefrontal correlates of monetary anticipation and outcome in chronic pain. Pain *159*, 1494–1507. https://doi.org/10.1097/j.pain.0000000000001232.

28. Apkarian, A.V., Baliki, M.N., and Farmer, M.A. (2013). Predicting transition to chronic pain. Curr. Opin. Neurol. *26*, 360–367. https://doi.org/10.1097/wco.0b013e32836336ad.

29. Redgrave, P., Gurney, K., and Reynolds, J. (2008). What is reinforced by phasic dopamine signals? Brain Res. Rev. *58*, 322–339. https://doi.org/10.1016/j.brainresrev.2007.10.007.

30. Chau, B.K., Jarvis, H., Law, C.-K., and Chong, T.T.-J. (2018). Dopamine and reward: a view from the prefrontal cortex. Behav. Pharmacol. *29*, 569–583. https://doi.org/10.1097/fbp.0000000000000424.

31. Schultz, W. (2016). Dopamine reward prediction-error signalling: a two-component response. Nat. Rev. Neurosci. *17*, 183–195. https://doi.org/10.1038/nrn.2015.26.

32. Jocham, G., Klein, T.A., and Ullsperger, M. (2011). Dopamine-mediated reinforcement learning signals in the striatum and ventromedial prefrontal cortex underlie value-based choices. J. Neurosci. *31*, 1606–1613. https://doi.org/10.1523/jneurosci.3904-10.2011.

33. Xie, J.Y., Qu, C., Patwardhan, A., Ossipov, M.H., Navratilova, E., Becerra, L., Borsook, D., and Porreca, F. (2014). Activation of mesocorticolimbic reward circuits for assessment of relief of ongoing pain: a potential biomarker of efficacy. PAIN® *155*, 1659–1666. https://doi.org/10.1016/j.pain.2014.05.018.

34. Baliki, M.N., Geha, P.Y., Fields, H.L., and Apkarian, A.V. (2010). Predicting value of pain and analgesia: nucleus accumbens response to noxious stimuli changes in the presence of chronic pain. Neuron *66*, 149–160. https://doi.org/10.1016/j.neuron.2010.03.002.

35. King, T., Vera-Portocarrero, L., Gutierrez, T., Vanderah, T.W., Dussor, G., Lai, J., Fields, H.L., and Porreca, F. (2009). Unmasking the tonic-aversive state in neuropathic pain. Nat. Neurosci. *12*, 1364–1366. https://doi.org/10.1038/nn.2407.

36. Chang, P.-C., Pollema-Mays, S.L., Centeno, M.V., Procissi, D., Contini, M., Baria, A.T., Martina, M., and Apkarian, A.V. (2014). Role of nucleus accumbens in neuropathic pain: linked multi-scale evidence in the rat transitioning to neuropathic pain. PAIN® *155*, 1128–1139. https://doi.org/10.1016/j.pain.2014.02.019.

37. Baliki, M.N., Mansour, A., Baria, A.T., Huang, L., Berger, S.E., Fields, H.L., and Apkarian, A.V. (2013). Parceling human accumbens into putative core and shell dissociates encoding of values for reward and pain. J. Neurosci. *33*, 16383–16393. https://doi.org/10.1523/jneurosci.1731-13.2013.

38. Day, J.J., Jones, J.L., and Carelli, R.M. (2011). Nucleus accumbens neurons encode predicted and ongoing reward costs in rats. Eur. J. Neurosci. *33*, 308–321. https://doi.org/10.1111/j.1460-9568.2010.07531.x.

39. Zhou, Z., Yu, R., and Zhou, X. (2010). To do or not to do? Action enlarges the FRN and P300 effects in outcome evaluation. Neuropsychologia *48*, 3606–3613. https://doi.org/10.1016/j.neuropsychologia.2010.08.010.

40. Elvemo, N., Landrø, N.I., Borchgrevink, P.C., and Håberg, A. (2015). Reward responsiveness in patients with chronic pain. Eur. J. Pain *19*, 1537–1543. https://doi.org/10.1002/ejp.687.

41. Wood, P.B., Patterson, J.C., II, Sunderland, J.J., Tainter, K.H., Glabus, M.F., and Lilien, D.L. (2007). Reduced presynaptic dopamine activity in fibromyalgia syndrome demonstrated with positron emission tomography: a pilot study. J. Pain *8*, 51–58. https://doi.org/10.1016/j.jpain.2006.05.014.

42. Martikainen, I.K., Nuechterlein, E.B., Pecina, M., Love, T.M., Cummiford, C.M., Green, C.R., Stohler, C.S., and Zubieta, J.-K. (2015). Chronic back pain is associated with alterations in dopamine neurotransmission in the ventral striatum. J. Neurosci. *35*, 9957–9965. https://doi.org/10.1523/jneurosci.4605-14.2015.

43. Hagelberg, N., Forssell, H., Rinne, J.O., Scheinin, H., Taiminen, T., Aalto, S., Luutonen, S., Någren, K., and Jääskeläinen, S. (2003). Striatal dopamine D1 and D2 receptors in burning mouth syndrome. Pain *101*, 149–154. https://doi.org/10.1016/s0304-3959(02)00323-8.

44. Grace, A.A., Floresco, S.B., Goto, Y., and Lodge, D.J. (2007). Regulation of firing of dopaminergic neurons and control of goal-directed behaviors. Trends Neurosci. *30*, 220–227. https://doi.org/10.1016/j.tins.2007.03.003.

45. Vlaeyen, J.W., and Crombez, G. (2020). Behavioral conceptualization and treatment of chronic pain. Annu. Rev. Clin. Psychol. *16*, 187–212. https://doi.org/10.1146/annurev-clinpsy-050718-095744.

46. Vlaeyen, J.W.S., Morley, S.J., Linton, S.J., Boersma, K., and Jong, J.d. (2012). Pain-Related Fear: Exposure-Based Treatment for Chronic Pain (IASP Press).

47. Flor, H., and Turk, D. (2011). Chronic Pain. An Integrated Biobehavioral Approach (IASP Press).

48. Ashar, Y.K., Gordon, A., Schubiner, H., Uipi, C., Knight, K., Anderson, Z., Carlisle, J., Polisky, L., Geuter, S., Flood, T.F., et al. (2022). Effect of pain reprocessing therapy vs placebo and usual care for patients with chronic back pain: a randomized clinical trial. JAMA Psychiatr. *79*, 13. https://doi.org/10.1001/jamapsychiatry.2021.2669.

49. Reckziegel, D., Tétreault, P., Ghantous, M., Wakaizumi, K., Petre, B., Huang, L., Jabakhanji, R., Abdullah, T., Vachon-Presseau, E., Berger, S., et al. (2021). Sex-specific pharmacotherapy for back pain: a

proof-of-concept randomized trial. Pain and therapy *10*, 1375–1400. https://doi.org/10.1007/s40122-021-00297-2.

50. Chen, A.L.-C., Chen, T.J., Waite, R.L., Reinking, J., Tung, H.L., Rhoades, P., Downs, B.W., Braverman, E., Braverman, D., Kerner, M., et al. (2009). Hypothesizing that brain reward circuitry genes are genetic antecedents of pain sensitivity and critical diagnostic and pharmacogenomic treatment targets for chronic pain conditions. Med. Hypotheses *72*, 14–22. https://doi.org/10.1016/j.mehy.2008.07.059.
51. Elliott, R., Newman, J.L., Longe, O.A., and William Deakin, J. (2004). Instrumental responding for rewards is associated with enhanced neuronal response in subcortical reward systems. Neuroimage *21*, 984–990. https://doi.org/10.1016/j.neuroimage.2003.10.010.
52. McClure, S.M., Berns, G.S., and Montague, P.R. (2003). Temporal prediction errors in a passive learning task activate human striatum. Neuron *38*, 339–346. https://doi.org/10.1016/s0896-6273(03)00154-5.
53. Hornak, J., O'doherty, J., Bramham, J., Rolls, E.T., Morris, R.G., Bullock, P.R., and Polkey, C.E. (2004). Reward-related reversal learning after surgical excisions in orbito-frontal or dorsolateral prefrontal cortex in humans. J. Cognit. Neurosci. *16*, 463–478. https://doi.org/10.1162/089892904322926791.
54. Domenech, P., Rheims, S., and Koechlin, E. (2020). Neural mechanisms resolving exploitation-exploration dilemmas in the medial prefrontal cortex. Science *369*, eabb0184. https://doi.org/10.1126/science.abb0184.
55. Lauwereyns, J., Watanabe, K., Coe, B., and Hikosaka, O. (2002). A neural correlate of response bias in monkey caudate nucleus. Nature *418*, 413–417. https://doi.org/10.1038/nature00892.
56. Faul, F., Erdfelder, E., Buchner, A., and Lang, A.-G. (2009). Statistical power analyses using G* Power 3.1: tests for correlation and regression analyses. Behav. Res. Methods *41*, 1149–1160. https://doi.org/10.3758/brm.41.4.1149.
57. Flor, H., Rudy, T.E., Birbaumer, N., Streit, B., and Schugens, M.M. (1990). Zur Anwendbarkeit des West Haven-Yale multidimensional pain inventory im deutschen Sprachraum. Schmerz *4*, 82–87. https://doi.org/10.1007/bf02527839.
58. Von Korff, M., Ormel, J., Keefe, F.J., and Dworkin, S.F. (1992). Grading the severity of chronic pain. Pain *50*, 133–149. https://doi.org/10.1016/0304-3959(92)90154-4.
59. Langenfeld, A., Bastiaenen, C., Brunner, F., and Swanenburg, J. (2018). Validation of the Orebro musculoskeletal pain screening questionnaire in patients with chronic neck pain. BMC Res. Notes *11*, 161. https://doi.org/10.1186/s13104-018-3269-x.
60. Herrmann, C., Buss, U., and Snaith, R. (1995). HADS-D Hospital Anxiety and Depression Scale—Ein Fragebogen zur Erfassung von Angst und Depressivität in der somatischen Medizin (Hans Huber).
61. Reis, D., Lehr, D., Heber, E., and Ebert, D.D. (2019). The German version of the Perceived Stress Scale (PSS-10): evaluation of dimensionality, validity, and measurement invariance with exploratory and confirmatory bifactor modeling. Assessment *26*, 1246–1259. https://doi.org/10.1177/1073191117715731.
62. Wittchen, H., Wunderlich, U., Gruschwitz, S., and Zaudig, M. (1997). SCID I: Structured Clinical Interview for DSM-IV. Axis I: Mental Disorders (SKID I. Strukturiertes Klinisches Interview Fur DSM-IV. Achse I: Psychische Storungen) (Hogrefe Publishers for Psychology).
63. Bradley, M.M., and Lang, P.J. (1994). Measuring emotion: the self-assessment manikin and the semantic differential. J. Behav. Ther. Exp. Psychiatr. *25*, 49–59. https://doi.org/10.1016/0005-7916(94)90063-9.
64. Yarkoni, T., Poldrack, R.A., Nichols, T.E., Van Essen, D.C., and Wager, T.D. (2011). Large-scale automated synthesis of human functional neuroimaging data. Nat. Methods *8*, 665–670. https://doi.org/10.1038/nmeth.1635.
65. Esteban, O., Markiewicz, C.J., Blair, R.W., Moodie, C.A., Isik, A.I., Erramuzpe, A., Kent, J.D., Goncalves, M., DuPre, E., Snyder, M., et al. (2018). fMRIPrep: a robust preprocessing pipeline for functional MRI. Nat. Methods *16*, 111–116. https://doi.org/10.1038/s41592-018-0235-4.
66. Esteban, O., Blair, R.W., Markiewicz, C.J., Berleant, S.L., Moodie, C.A., Ma, F., Isik, A.I., Erramuzpe, A., Kent, J.D., Goncalves, M., and DuPre, E.. "FMRIPrep." Software. Zenodo. https://doi.org/10.5281/zenodo.852659.
67. Gorgolewski, K.J., Esteban, O., Markiewicz, C.J., Ziegler, E., Ellis, D.G., Notter, M.P., Jarecka, D., Johnson, H., Burns, C., and Manhães-Savio, A. (2018). Nipype. Software. Zenodo. https://doi%20org/10.5281/zenodo%20596855.
68. Ghosh, S.S., Waskom, M.L., Halchenko, Y.O., Clark, D., Madison, C., Burns, C.D., and Gorgolewski, K. (2011). Nipype: a flexible, lightweight and extensible neuroimaging data processing framework in Python. Front. Neuroinf. *5*, 13. https://doi.org/10.3389/fninf.2011.00013.
69. Tustison, N.J., Avants, B.B., Cook, P.A., Yuanjie, Z., Egan, A., Yushkevich, P.A., and Gee, J.C. (2010). N4ITK: improved N3 bias correction. IEEE Trans. Med. Imag. *29*, 1310–1320. https://doi.org/10.1109/tmi.2010.2046908.
70. Avants, B.B., Epstein, C.L., Grossman, M., and Gee, J.C. (2008). Symmetric diffeomorphic image registration with cross-correlation: evaluating automated labeling of elderly and neurodegenerative brain. Med. Image Anal. *12*, 26–41. https://doi.org/10.1016/j.media.2007.06.004.
71. Zhang, Y., Brady, M., and Smith, S. (2001). Segmentation of brain MR images through a hidden Markov random field model and the expectation-maximization algorithm. IEEE Trans. Med. Imag. *20*, 45–57. https://doi.org/10.1109/42.906424.
72. Fonov, V.S., Evans, A.C., McKinstry, R.C., Almli, C.R., and Collins, D.L. (2009). Unbiased nonlinear average age-appropriate brain templates from birth to adulthood. Neuroimage *47*, S102. https://doi.org/10.1016/s1053-8119(09)70884-5.
73. Glasser, M.F., Sotiropoulos, S.N., Wilson, J.A., Coalson, T.S., Fischl, B., Andersson, J.L., Xu, J., Jbabdi, S., Webster, M., Polimeni, J.R., et al. (2013). The minimal preprocessing pipelines for the Human Connectome Project. Neuroimage *80*, 105–124. https://doi.org/10.1016/j.neuroimage.2013.04.127.
74. Jenkinson, M., and Smith, S. (2001). A global optimisation method for robust affine registration of brain images. Med. Image Anal. *5*, 143–156. https://doi.org/10.1016/s1361-8415(01)00036-6.
75. Greve, D.N., and Fischl, B. (2009). Accurate and robust brain image alignment using boundary-based registration. Neuroimage *48*, 63–72. https://doi.org/10.1016/j.neuroimage.2009.06.060.
76. Jenkinson, M., Bannister, P., Brady, M., and Smith, S. (2002). Improved optimization for the robust and accurate linear registration and motion correction of brain images. Neuroimage *17*, 825–841. https://doi.org/10.1006/nimg.2002.1132.
77. Cox, R.W., and Hyde, J.S. (1997). Software tools for analysis and visualization of fMRI data. NMR Biomed. *10*, 171–178. https://doi.org/10.1002/(sici)1099-1492(199706/08)10:4/5<171::aid-nbm453>3.0.co;2-l.
78. Power, J.D., Mitra, A., Laumann, T.O., Snyder, A.Z., Schlaggar, B.L., and Petersen, S.E. (2014). Methods to detect, characterize, and remove motion artifact in resting state fMRI. Neuroimage *84*, 320–341. https://doi.org/10.1016/j.neuroimage.2013.08.048.
79. Behzadi, Y., Restom, K., Liau, J., and Liu, T.T. (2007). A component based noise correction method (CompCor) for BOLD and perfusion based fMRI. Neuroimage *37*, 90–101. https://doi.org/10.1016/j.neuroimage.2007.04.042.
80. Satterthwaite, T.D., Elliott, M.A., Gerraty, R.T., Ruparel, K., Loughead, J., Calkins, M.E., Eickhoff, S.B., Hakonarson, H., Gur, R.C., Gur, R.E., and Wolf, D.H. (2013). An improved framework for confound regression and filtering for control of motion artifact in the preprocessing of resting-state functional connectivity data. Neuroimage *64*, 240–256. https://doi.org/10.1016/j.neuroimage.2012.08.052.

81. Lanczos, C. (1964). Evaluation of noisy data. J. Soc. Ind. Appl. Math. B Numer. Anal. *1*, 76–85. https://doi.org/10.1137/0701007.

82. Abraham, A., Pedregosa, F., Eickenberg, M., Gervais, P., Mueller, A., Kossaifi, J., Gramfort, A., Thirion, B., and Varoquaux, G. (2014). Machine learning for neuroimaging with scikit-learn. Front. Neuroinf. *8*, 14. https://doi.org/10.3389/fninf.2014.00014.

83. Woolrich, M.W., Ripley, B.D., Brady, M., and Smith, S.M. (2001). Temporal autocorrelation in univariate linear modeling of FMRI data. Neuroimage *14*, 1370–1386. https://doi.org/10.1006/nimg.2001.0931.

84. Mason, S.J., and Graham, N.E. (2002). Areas beneath the relative operating characteristics (ROC) and relative operating levels (ROL) curves: statistical significance and interpretation. Q. J. R. Meteorol. Soc. *128*, 2145–2166. https://doi.org/10.1256/003590002320603584.

85. Imai, K., Keele, L., Tingley, D., and Yamamoto, T. (2010). Causal mediation analysis using R. In Advances in social science research using R (Springer), pp. 129–154.

86. Oosterhof, N.N., Connolly, A.C., and Haxby, J.V. (2016). CoSMoMVPA: multi-modal multivariate pattern analysis of neuroimaging data in Matlab/GNU Octave. Front. Neuroinf. *10*, 27. https://doi.org/10.3389/fninf.2016.00027.

87. Haxby, J.V., Gobbini, M.I., Furey, M.L., Ishai, A., Schouten, J.L., and Pietrini, P. (2001). Distributed and overlapping representations of faces and objects in ventral temporal cortex. Science *293*, 2425–2430. https://doi.org/10.1126/science.1063736.

88. Winkler, A.M., Ridgway, G.R., Webster, M.A., Smith, S.M., and Nichols, T.E. (2014). Permutation inference for the general linear model. Neuroimage *92*, 381–397. https://doi.org/10.1016/j.neuroimage.2014.01.060.

STAR★METHODS

KEY RESOURCES TABLE

REAGENT or RESOURCE	SOURCE	IDENTIFIER
Software and algorithms		
FSL 6.0.0	Oxford Centre for Functional MRI of the Brain	https://fsl.fmrib.ox.ac.uk/fsldownloads_registration; RRID:SCR_002823
FSL 5.0.11	Oxford Centre for Functional MRI of the Brain	https://fsl.fmrib.ox.ac.uk/fsldownloads_registration; RRID:SCR_002823
JASP 0.14.1.0	University of Amsterdam	https://github.com/jasp-stats/jasp-desktop; RRID:SCR_015823
fMRIprep 20.0.7	Poldrack Lab	https://fmriprep.org/en/stable/; RRID: SCR_016216
CoSMoMVPA	https://www.cosmomvpa.org/	https://github.com/CoSMoMVPA/CoSMoMVPA; RRID:SCR_014519

RESOURCE AVAILABILITY

Lead contact

Requests for resources should be directed to and will be fulfilled by the lead contact, Martin Löffler (Martin.Loeffler@zi-mannheim.de).

Materials availability

This study did not generate new unique reagents.

Data and code availability

- All data reported in this paper will be shared by the lead contact upon request.
- This paper does not report the original code.
- Any additional information required to reanalyze the data reported in this paper is available from the lead contact upon request.

EXPERIMENTAL MODEL AND SUBJECT DETAILS

Subjects

Participants were recruited through the outpatient pain clinic of the Institute of Cognitive and Clinical Neuroscience, general practitioners, and physiotherapy practices as well as reports in local newspapers and through the institute's website. We examined fifty patients with subacute back pain, 29 patients with chronic back pain and 29 healthy controls. Patients with CBP and controls were matched for age and gender. Bayesian null-hypothesis testing with Jeffreys's Amazing Statistics Program (JASP) version 0.14.0.0 and zero-centered standard medium-width priors showed anecdotal to moderate evidence for the null hypotheses, i.e. confirmed that the age of patients with CBP did not differ from controls BF_{01} = 2.973) and that gender of patients with CBP did not differ from controls (BF_{01} = 3.078). To meet inclusion criteria, participants had to be at least 18 years old. Healthy controls were included only if they were free of pain. For the SABP group we included patients with a current back pain episode of 7–12 weeks of back pain. Patients with a current back pain episode and additional back pain episodes in their history were included as well, if the episodes never exceeded a period of 12 weeks. For the CBP group we only included patients with a current back pain episode of more than 100 days. For participant characteristics, see Table 1. Current and past medication was assessed as self-report prior to the experiment. Regular use was reported for NSAIDs (5 SABP, 3 CBP), statins (1 CBP), antihistamines (1 CBP) angiotensin receptor blockers (2 SABP), and proton-pump inhibitors (1 SABP). Occasional use was reported for NSAIDs (1 HC, 2 SABP, 3 CBP), antihistamines (1 HC, 1 CBP), angiotensin receptor blockers (1 CBP) and benzodiazepines (1 CBP). Past medication was reported for NSAIDs (1 HC, 22 SABP, 14 CBP), opiates (2 CBP), ACE inhibitors (1 CBP), benzodiazepines (1 SABP, 2 CBP) and cannabinoids (1 SABP).

Patients were assessed for general eligibility via self-report using a screening intake form, which covered co-morbid health and psychological conditions, MRI safety, concomitant medication dosages and indications, current and previous illicit drug/alcohol use, and pain levels. All participants passed the MRI safety screening requirements at each scanning visit. Informed consent was obtained from all participants on their first visit. Participants were compensated with €10/hour. All procedures were approved by the Ethics Committee of the Medical Faculty Mannheim of Heidelberg University and complied with the Declaration of Helsinki in its most recent form. One patient with SABP was unavailable for the follow-up screening and therefore dropped out at follow-up,

and one additional patient with SABP was excluded as an outlier because of an extreme increase in pain severity from baseline to follow-up (466 percent, at a sample mean of −15.62 percent the subject was >6 standard deviations from the sample mean). We could not acquire resting state scans from four patients with SABP, two patients with CBP and four HC.

We based our sample size calculation on the expected correlation between extracted beta values from the univariate analysis at baseline and the change in pain severity from baseline to follow-up. Previous publications found high correlations between NAc connectivity and pain measures at baseline (between r = 0.72 and r = 0.76[8] and r = 0.86[34]). We therefore expected a moderate to high correlation of NAc connectivity with change in pain severity. *A priori* sample size estimation with GPower 3.1.9.2[56] for an *a priori* sample size calculation with an expected correlation of r = 0.7, a power of 0.90 and a p of 0.05, which was adjusted for multiple comparisons with 3 regions of interest, 9 contrasts of interest (i.e. 27 tests) and task-based functional connectivity between vmPFC and bilateral NAc for the 9 contrasts of interest (i.e. 18 tests), resulting in a corrected threshold of p = 0.001 and a required sample size of 27 patients. This is an interim evaluation of a larger ongoing project.

Clinical assessments

We employed the percentage change in the Pain Severity scale of the German version of the West Haven-Yale Multidimensional Pain Inventory at the beginning of the baseline assessment[57] to the follow-up screening after 6 months using the following formula: $\Delta PS = \frac{PS_{follow-up} - PS_{baseline}}{PS_{baseline}} \times 100$ as an indicator of pain persistence.

At the beginning of the baseline assessment, the participants additionally completed the German versions of the Chronic Pain Grade (CPG),[58] the Örebro Musculoskeletal Pain Questionnaire (YF),[59] the Hospital Anxiety and Depression Scale (HADS),[60] and the Perceived Stress Scale (PSS).[61] All sample characteristics are depicted in Table 1.

To assess comorbid mental disorders, all participants were interviewed by a psychologist using the German version of the Structured Clinical Interviews (SCID I) for the Diagnostic and Statistical Manual of Mental Disorders (DSM IV),[62] see Table S1 for all current or past disorders.

METHOD DETAILS

Experimental procedures

A differential operant conditioning paradigm was carried out during fMRI. Participants were able to win money (1€) or pain relief (reduce pain duration from 3 to 1.5 s) via button presses in response to two colored arrows that served as discriminative stimuli (DS). The color (blue/yellow) of the arrows indicated the type of potential reward. Reward was not given if participants reacted too slowly (>6 s). In all other trials the reinforcement rate was predefined, and participants received the respective reward with a 50% reinforcement schedule. Discriminative stimuli were presented for 6 s, followed by an anticipation phase (4 s), and the feedback phase. In the monetary reward condition, an image of a 1€ coin was presented during the entire feedback phase (3 s). In the pain relief condition the painful stimulus was always presented for 1.5 s and continued for another 1.5 s in trials without pain relief, whereas it stopped after 1.5 s in pain relief trials. The inter trial interval was randomly jittered between 8 and 10 s, see Figure 1.

For stimulus delivery Presentation® software (Version 18.3, http://www.neurobs.com/) was used. Visual stimuli were presented to the subjects via goggles. Painful stimuli were applied via copper surface electrodes at the left thumb with a stimulus duration of 2 ms and at a frequency of 12 Hz, using a constant current stimulator (model DS7A; Digitimer, Hertfordshire, England). Prior to the experiment, the stimulus intensity was calibrated to a perceived pain intensity rating of 7-8 on a numeric rating scale (endpoints 0 = "no pain" and 10 = "worst pain imaginable"). This stimulus intensity was used for all further procedures (stimulus intensities used were HC: mean = 6.32 mA, standard deviation = 5.29 mA; CBP: mean = 5.30 mA, standard deviation = 7.27 mA; SABP: mean = 5.46 mA, standard deviation = 4.55 mA).

The experiment consisted of three phases. During habituation participants would undergo 8 trials of each type, but without monetary reward, pain, or pain relief. The acquisition phase consisted of 20 trials of each condition. During extinction DS_{money} and $DS_{painrelief}$ were presented 8 times again, but without painful stimulation, pain relief or monetary reward. At the end of each phase participants performed ratings of perceived valence, pain, and contingency of the discriminative stimuli. Ratings of valence and arousal were assessed using the self-assessment manikins,[63] asking: "How pleasant/unpleasant was the blue/yellow arrow?" and "How arousing did you find the blue/yellow arrow?". They were later converted to a 1 to 9 scale. Contingency ratings were given on a scale from 1 to 9, asking "How likely was the blue/yellow arrow followed by a monetary reward/painful relief?", ranging from "highly unlikely" to "highly likely". We employed separate analyses of variance to test main effects of group (persistent versus recovered patients with SABP or CBP versus HC respectively) and interaction effects for group and phase (habituation versus acquisition versus extinction). None of these variables significantly differed between CBP and controls or patients with persistent and recovered SABP. Additionally, we correlated the changes in perceived valence/arousal/contingency and reaction times from habituation to acquisition and from acquisition to extinction with the change in pain severity (in patients with SABP), or the pain severity at baseline (in patients with CBP). None of these parameters showed any significant association with severity of pain (CBP) or changes in pain severity (SABP), see Tables S2 and S3 and Figures S1, S2, S3, and S4).

Magnetic resonance imaging

Magnetic resonance imaging was performed on a 3 Tesla Tim TRIO whole body scanner (SIEMENS Healthineers, Erlangen, Germany), equipped with a 12-channel head coil. For visual presentation we used goggles (see above). To be able to comfortably fit

these into the head coil for participants with large head sizes we used a 12-channel head coil. Shimming of the scanner was done to account for maximum magnetic field homogeneity and a standard gradient field map was recorded at the beginning of each measurement.

For the task-based functional protocol, 40 contiguous axial slices (slice thickness: 2.3 mm, slice gap: 0.7 mm) were acquired using a T2*-weighted gradient-echo echo-planar imaging (EPI) sequence with GRAPPA technique (acceleration factor 2, repetition time (TR) = 2350 ms, echo time (TE) = 22 ms, matrix size = 96 × 96, field of view (FoV) = 220 × 220 mm^2, flip angle (α) = 90°, bandwidth (BW) = 1270 Hz/px).

For the resting-state functional protocol, 36 contiguous axial slices (slice thickness: 3 mm, slice, in-plain voxel size: 2.3 × 2.3 mm, no gap) were acquired using a T2*-weighted gradient-echo echo-planar imaging (EPI) sequence with GRAPPA technique (acceleration factor 2, repetition time (TR) = 2100 ms, echo time (TE) = 23 ms, matrix size = 96 × 96, field of view (FoV) = 220 × 220 mm2, flip angle (α) = 90°, bandwidth (BW) = 1370 Hz/px). Two-hundred-and ten volumes were acquired in a total of 7 min and 21 s. Resting-state scans were acquired on a separate experimental day. Subjects were asked to lay still with their eyes closed, remain awake and try not to think about anything specific.

For structural reference, we used a T1-weighted magnetization prepared rapid gradient echo (MPRAGE) sequence (TR = 2300 ms, TE = 2.98 ms, matrix size = 240 × 256, field of view (FoV) = 240 × 256 mm2, flip angle (α) = 9°, bandwidth (BW) = 240 Hz/px) recording with 192 sagittal slices.

Regions of interest

Masks for bilateral NAc and vmPFC for task-based and resting state fMRI were identified by extracting uniformity maps from the meta-analysis tool Neurosynth.org,[64] which identified 194 PubMed studies for the term ''nucleus accumbens'' and 333 PubMed studies for the term ''ventromedial prefrontal'' (as of January 2021). Individual thresholds of these maps were determined by visual inspection, to cover the anatomical region as well as possible. Final thresholds were z values larger than 20 for NAc and larger than 10 for vmPFC. Afterwards, the maps were corrected manually for voxels not belonging to the respective regions but representing voxels of associated regions as defined by the meta-analysis tool. Finally, the NAc mask was split up into separate masks for right and left NAc.

QUANTIFICATION AND STATISTICAL ANALYSIS

Preprocessing of magnetic resonance imaging data

Results included in this manuscript come from preprocessing performed using fMRIPrep version 20.0.7. The following boilerplate text was automatically generated by fMRIPrep:

Results included in this manuscript come from preprocessing performed using fMRIPrep 20.0.7,[65,66] which is based on Nipype 1.4.2.[67,68]

Anatomical data preprocessing

The T1-weighted (T1w) image was corrected for intensity non-uniformity (INU) with N4BiasFieldCorrection,[69] distributed with ANTs 2.2.0,[70] and used as T1w-reference throughout the workflow. The T1w-reference was then skull-stripped with a Nipype implementation of the antsBrainExtraction.sh workflow (from ANTs), using OASIS30ANTs as target template. Brain tissue segmentation of cerebrospinal fluid (CSF), white-matter (WM) and gray-matter (GM) was performed on the brain-extracted T1w using fast (FSL 5.0.9[71]). Volume-based spatial normalization to one standard space (MNI152NLin2009cAsym) was performed through nonlinear registration with antsRegistration (ANTs 2.2.0), using brain-extracted versions of both T1w reference and the T1w template. The following template was selected for spatial normalization: ICBM 152 Nonlinear Asymmetrical template version 2009c[72] TemplateFlow ID: MNI152NLin2009cAsym.

Functional data preprocessing

For each of the 4 BOLD runs found per subject (across all tasks and sessions), the following preprocessing was performed. First, a reference volume and its skull-stripped version were generated using a custom methodology of fMRIPrep. A B0-nonuniformity map (or fieldmap) was estimated based on a phase-difference map calculated with a dual-echo GRE (gradient-recall echo) sequence, processed with a custom workflow of SDCFlows inspired by the epidewarp.fsl script (http://www.nmr.mgh.harvard.edu/greve/fbirn/b0/epidewarp.fsl) and further improvements in HCP Pipelines.[73] The fieldmap was then co-registered to the target EPI (echo-planar imaging) reference run and converted to a displacements field map (amenable to registration tools such as ANTs) with FSL's fugue and other SDCflows tools. Based on the estimated susceptibility distortion, a corrected EPI (echo-planar imaging) reference was calculated for a more accurate co-registration with the anatomical reference. The BOLD reference was then co-registered to the T1w reference using flirt (FSL 5.0.9[74]) with the boundary-based registration[75] cost-function. Co-registration was configured with nine degrees of freedom to account for distortions remaining in the BOLD reference. Head-motion parameters with respect to the BOLD reference (transformation matrices, and six corresponding rotation and translation parameters) are estimated before any spatiotemporal filtering using mcflirt (FSL 5.0.9[76]). BOLD runs were slice-time corrected using 3dTshift from AFNI 20160207.[77] The BOLD time-series (including slice-timing correction when applied) were resampled onto their original, native space by applying a

single, composite transform to correct for head-motion and susceptibility distortions. These resampled BOLD time-series will be referred to as preprocessed BOLD in original space, or just preprocessed BOLD. The BOLD time-series were resampled into standard space, generating a preprocessed BOLD run in MNI152NLin2009cAsym space. First, a reference volume and its skull-stripped version were generated using a custom methodology of fMRIPrep. Several confounding time-series were calculated based on the preprocessed BOLD: framewise displacement (FD), DVARS and three region-wise global signals. FD and DVARS are calculated for each functional run, both using their implementations in Nipype (following the definitions by Power et al.[78]). The three global signals are extracted within the CSF, the WM, and the whole-brain masks. Additionally, a set of physiological regressors were extracted to allow for component-based noise correction (CompCor[79]). Principal components are estimated after high-pass filtering the preprocessed BOLD time-series (using a discrete cosine filter with 128 s cut-off) for the two CompCor variants: temporal (tCompCor) and anatomical (aCompCor). tCompCor components are then calculated from the top 5% variable voxels within a mask covering the subcortical regions. This subcortical mask is obtained by heavily eroding the brain mask, which ensures it does not include cortical GM regions. For aCompCor, components are calculated within the intersection of the aforementioned mask and the union of CSF and WM masks calculated in T1w space, after their projection to the native space of each functional run (using the inverse BOLD-to-T1w transformation). Components are also calculated separately within the WM and CSF masks. For each CompCor decomposition, the k components with the largest singular values are retained, such that the retained components' time series are sufficient to explain 50 percent of variance across the nuisance mask (CSF, WM, combined, or temporal). The remaining components are dropped from consideration. The head-motion estimates calculated in the correction step were also placed within the corresponding confounds file. The confound time series derived from head motion estimates and global signals were expanded with the inclusion of temporal derivatives and quadratic terms for each.[80] Frames that exceeded a threshold of 0.5 mm FD or 1.5 standardized DVARS were annotated as motion outliers. All resamplings can be performed with *a single interpolation step* by composing all the pertinent transformations (i.e. head-motion transform matrices, susceptibility distortion correction when available, and co-registrations to anatomical and output spaces). Gridded (volumetric) resamplings were performed using antsApplyTransforms (ANTs), configured with Lanczos interpolation to minimize the smoothing effects of other kernels.[81] Non-gridded (surface) resamplings were performed using mri_vol2surf (FreeSurfer).

Many internal operations of fMRIPrep use Nilearn 0.6.2,[82] mostly within the functional processing workflow. For more details of the pipeline, see the section corresponding to workflows in fMRIPrep's documentation.

The above boilerplate text was automatically generated by fMRIPrep with the express intention that users should copy and paste this text into their manuscripts *unchanged*. It is released under the creative commons (https://creativecommons.org/publicdomain/zero/1.0/) license.

Outlier detection, imputation, and correction for multiple comparisons

Observations with a Cook's distance of 4/(n – k - 1), where n is the sample size and k is the number of independent variables, were defined as influential outliers and removed from the respective analysis. Missing values were imputed using the MICE package version 3.13.0, in R, applying predictive mean matching for numeric variables and a proportional odds model for ordered variables.

All tests are reported with Bonferroni-corrected p values.

Reward learning and the transition to chronic pain: ROI and connectivity analysis

FMRI data processing was carried out using FEAT (FMRI Expert Analysis Tool) Version 6.00, part of FSL (FMRIB's Software Library, www.fmrib.ox.ac.uk/fsl). The first 3 volumes were discarded to account for scanner saturation effects. The following pre-statistics processing was applied: spatial smoothing using a 5-mm full width at half maximum Gaussian blur (only for univariate analyses, not for multivariate pattern analysis), grand-mean intensity normalization of the entire 4D dataset by a single multiplicative factor. Time-series statistical analysis was carried out using FILM with local autocorrelation correction[83] with nine regressors of interest: 1) DS_{money}, 2) $DS_{pain\ relief}$, 3) $anticipation_{money}$, 4) $anticipation_{pain\ relief}$, 5) feedback money without reward (NPE_{money}: negative prediction error money), 6) feedback money with reward (PPE_{money}: positive prediction error money), 7) feedback pain relief with pain ($NPE_{pain\ relief}$: negative prediction error pain relief) 8) feedback pain relief without pain ($PPE_{pain\ relief}$: positive prediction error pain relief) 9) US_{pain}. DS_{money} and $DS_{pain\ relief}$ were modelled as the entire 6 s of the presentation of the respective stimulus. $Anticipation_{money}$ and $anticipation_{pain\ relief}$ were modelled as the entire 4 s between the respective discriminative stimulus and the onset of the US_{pain} or NPE_{money}/PPE_{money}. PPE_{money} was modelled as the entire 3 s of the presentation of the monetary reward and NPE_{money} as the 3 s during the same time period, but when no monetary reward was presented. US_{pain} was modeled as the first 1.5 s of painful stimulus that were always presented in the pain relief condition. $PPE_{pain\ relief}$ was modelled as the absence of pain during the 1.5 s following the US_{pain}. $NPE_{pain\ relief}$ was modelled during the 1.5 s after the US_{pain} in case of persistent pain.

We included nuisance regressors for framewise displacement (FD), global signal, and the first five white matter and first five CSF components derived from CompCor regressors for white matter signal and five CompCor regressors for CSF signal, for time points that exceeded a threshold of 0.5 mm FD or 1.5 standardized DVARS, as extracted by fMRIPrep (see above). BOLD signals (parameter estimates) were extracted for the three regions of interest left NAc, right NAc and vmPFC for each participant. A psychophysiological interaction analysis (PPI) was used to determine which voxels in the bilateral NAc alter their relationship (connectivity) with a seed region of interest (the vmPFC) in a given condition. PPI parameter estimates were extracted from the left and right NAc for each participant.

To predict the transition from subacute to chronic pain, parameter estimates extracted from vmPFC and left and right NAc, as well as PPI parameter estimates extracted from left and right NAc, were correlated with the percentage change in pain severity ($\Delta PS = \frac{PS_{follow-up} - PS_{baseline}}{PS_{baseline}} \times 100$) from baseline to the 6 months follow-up. To show a measure of sensitivity and specificity and to allow for comparisons to previous work,[8] which binarized the data to patients with pain that persisted over time ($\Delta PS > -20\%$, n = 21) and patients that recovered ($\Delta PS < -20\%$, n = 27), we followed this procedure with a classification analysis. We present receiver operating characteristic (ROC) curves with recovered and persistent pain patients as binary classes and the respective parameter estimates as classifying variable. The area underneath each ROC curve was calculated following the process outlined in Mason and Graham,[84] with a p value calculated using the Wilcoxon test addressing the null hypothesis that the area under the ROC curve is 0.5 (i.e. the forecast is not predictive).

Resting-state prediction of the transition to chronic pain

Resting state scans were preprocessed, using the same pipeline and nuisance regressors as for the task-based scans. Additionally, we applied a low-pass filter at 0.2 Hz using the fslmaths function of FSL version 5.0.11. Time series were extracted for each participant from the three regions of interest. Pearson's correlation between time series of the vmPFC and bilateral NAc were used to derive an estimate of functional connectivity at rest.

We additionally tested if the task-based prediction of chronicity was mediated by resting-state connectivity between vmPFC and lNAc/rNAc by carrying out mediation analyses using the "mediation" package version 4.5.0, in R.[85] Unstandardized indirect effects were computed for each of 1′000 bootstrapped samples, and the 95% confidence interval was computed by determining the indirect effects at the 2.5 th and 97.5th percentiles.

Reward learning and the transition to chronic pain: Pattern decoding

With the goal of predicting the eventual recovery status of the patients with subacute back pain from cortical activity patterns, we additionally used the CoSMoMVPA toolbox[86] to carry out multivariate pattern analysis (MVPA)[87] in our three regions of interest (vmPFC, left NAc and right NAc). Within a given region, we trained a linear discriminant analysis (LDA) classifier on the mean-centered multivoxel patterns of t-scores from the unsmoothed first-level contrasts of interest (1. DS_{money}, 2. $DS_{pain\ relief}$, 3. anticipation money, 4. anticipation pain relief, 5. negative prediction error money, 6. positive prediction error money, 7. negative prediction error pain relief 8. positive prediction error pain relief 9. US_{pain}) that corresponded to these labels for all but two patients (i.e., one recovered and one persistent patient) and then tested the classifier on the activity patterns of these two left-out patients. This procedure was repeated via exhaustive cross-validation of splitting the 48 patients into all possible unique training sets of 46 and the corresponding test sets of 2 (always ensuring that the test set contained one recovered and one persistent patient), which yielded 567-folds. The same procedure was carried out for the pattern of functional connectivity to the vmPFC in the bilateral NAc. Subject-wise accuracy was extracted as the average accuracy across folds for a given subject. We created receiver operating characteristic (ROC) curves for the individual probability (across folds) of being classified as a persistent patient. The respective area under the curve was tested against chance level (see above).

Reward learning characteristics in chronic back pain

To check whether neural representations of reward learning that predicted chronicity are specific for the transition from acute to chronic pain or persist in the chronic stage, we employed permutation testing to reveal locations within a mask of vmPFC and bilateral NAc, where BOLD differed between HC and CBP (non-parametric two-samples t-test using 'randomize' function;[88] 5,000 permutations). Family-wise error rate was controlled using threshold-free cluster enhancement as implemented in FSL ($p < 0.05$). In patients with CBP, we additionally extracted parameter estimates from vmPFC and left and right NAc as well as PPI parameter estimates from left and right NAc and correlated them with pain severity as assessed by the West Haven-Yale Multidimensional Pain Inventory. To show a measure of sensitivity and specificity for the classification of controls versus patients with CBP, we followed the same procedure as for the binary classification approach of patients with persistent SABP and patients with SABP who recovered, presenting ROC curves classifying controls and patients with CBP.

For the resting state scans, the same procedure that was used to identify patients with SABP that develop chronic pain was applied to test if vmPFC-NAc functional connectivity at rest distinguishes between patients with chronic pain (n = 27) and controls (n = 25) and if the pain severity of these patients was associated with higher vmPFC-NAc connectivity.

ADDITIONAL RESOURCES

The study has been registered on the "German Clinical Trials Register" the registration ID is DRKS00008835. The access website is as follows: https://www.drks.de/.

Cell Reports Medicine, Volume *3*

Supplemental information

Corticostriatal circuits in the transition to chronic back pain: The predictive role of reward learning

Martin Löffler, Seth M. Levine, Katrin Usai, Simon Desch, Mina Kandić, Frauke Nees, and Herta Flor

	Code	Diagnoses	Remitted	Acute
SABP	296.26	Major depressive disorder, single episode	10	
	296.30/296.36	Major depressive disorder, recurrent	2	2
	300.29	Specific phobia		1
	300.3	Obsessive-compulsive disorder	1	
	303.90	Dependence: Alcohol	2	
	304.xx	Dependence: Cannabis, Cocaine, Opioids	2	
	305.xx	Abuse: Opioids/Amphetamine/Cannabis/ Sedative-, hypnotic-, or anxiolytic-related	3	1
	307.51	Bulimia Nervosa	1	
	309.81	Posttraumatic stress disorder	1	
HC	296.26	Major depressive disorder, single episode	1	
CBP	296.26	Major depressive disorder, single episode	3	
	296.33/296.36	Major depressive disorder, recurrent	3	2
	300.01	Panic disorder, without agoraphobia		2
	300.22	Agoraphobia without history of panic disorder	1	
	303.90	Dependenc: Alcohol	1	
	304.10	Dependence: Sedative-, hypnotic-, or anxiolytic-related	1	
	305.xx	Abuse: Cannabis, Cocaine, Hallucinogen, Amphetamine	1	
	307.10	Anorexia Nervosa		1
	307.51	Bulimia Nervosa	1	

Supplementary table 1 reports comorbid metal disorders. Related to STAR Methods: diagnoses according to the Diagnostic and Statistical Manual of Mental Disorders IV (DSM IV) in controls (HC), patients with chronic back pain (CBP) and patients with subacute back pain (SABP)

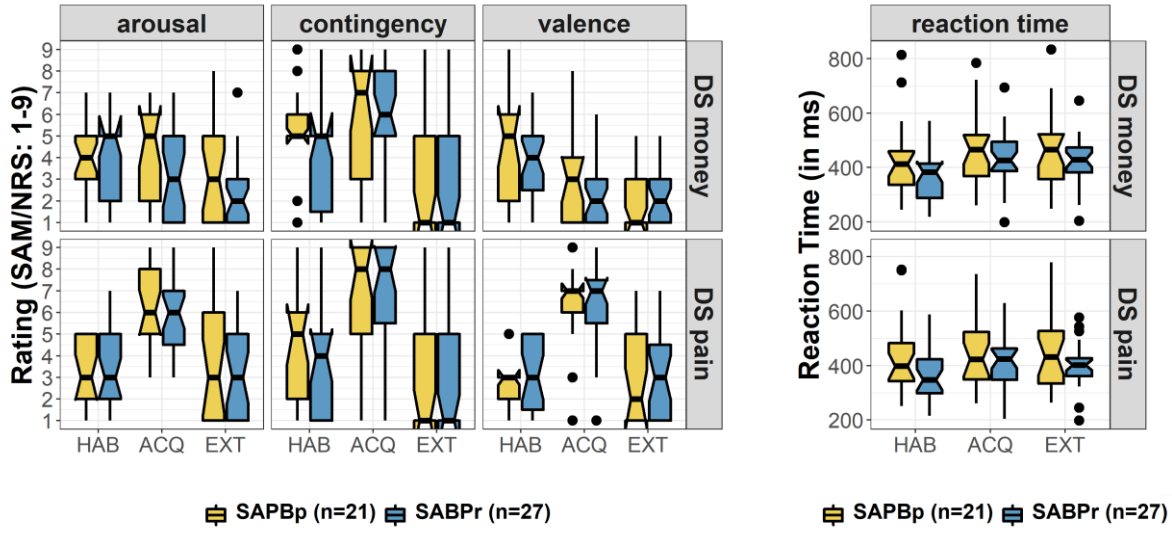

Supplementary Figure 1 depicts ratings and reaction times of patients with remitted and persistent SABP. Related to STAR Methods: *Boxplots show patients with remitted pain (SABPr, yellow) and persistent pain (SABPp, blue) at 6 months follow-up. Ratings of valence and arousal were assessed on a scale from 1 to 9 using the self-assessment manikins. Higher values indicate higher perceived arousal/valence/contingency. Abbreviations: DS: discriminative stimulus; HAB: habituation; ACQ: acquisition; EXT: extinction; SAM: Self-Assessment Manikin; NRS: Numeric Rating Scale; ms: milliseconds;*

Analyses of perceived arousal, valence and contingency and reaction times to DS_{money} and $DS_{pain\ relief}$ in patients with persistent SABP and recovered SABP

		F-Tests			Posthoc-tests: SABP persistent		Posthoc-tests: SABP recovered	
		Group (SABPr – SABPp): F(df); p; ges	**Phase (HAB-ACQ-EXT): F(df); p; ges**	**Group x Phase F(df); p; ges**	**HAB-ACQ t(df); p; d**	**ACQ-EXT t(df); p; d**	**HAB-ACQ t(df); p; d**	**ACQ-EXT t(df); p; d**
DS_{money}	**Arousal**	F(1,46)=1.93; p=0.171; ges=0.020	**F(1.76,80.79)=7.25; p=0.002; ges=0.076**	F(1.76,80.79)=1.33; p=0.269; ges=0.015	t(20)=-1.02; p=0.96; d=-0.222	t(20)=2.57; p=0.054; d=0.562	t(26)=0.89; p=1.000; d=0.171	**t(26)=2.98; p=0.018; d=0.574**
	Valence	F(1,46)=0.61; p=0.441; ges=0.006	**F(1.55,71.1)=18.10; p<0.001; ges=0.171**	F(1.55,71.1)=0.69; p=0.472; ges=0.008	t(20)=2.09; p=0.150; d=0.455	t(20)=2.27; p=0.103; d=0.496	**t(26)=3.49; p=0.005; d=0.671**	t(26)=0.38; p=1.000; d=0.074
	Contingency	F(1,46)=0.095; p=0.759; ges<0.001	**F(1.68,77.31)=16.32; p<0.001; ges=0.174**	F(1.68,77.31)=1.10; p=0.330; ges=0.014	t(20)=-0.953; p=1.000; d=-0.208	**t(20)=2.96; p=0.023; d=0.646**	**t(26)=-3.72; p=0.003; d=-0.717**	**t(26)=3.97; p=0.002; d=0.763**
	Reaction time	F(1,46)=1.48; p=0.230; ges=0.028	**F(1.6,73.41)=15.65; p<0.001; ges=0.032**	F(1.6,73.41)=0.84; p=0.413; ges=0.002	t(20)=-2.31; p=0.095; d=-0.504	t(20)=0.43; p=1.000; d=0.093	**t(26)=-4.09; p=0.001; d=-0.787**	t(26)=2.02; p=0.16; d=0.389
$DS_{pain\ relief}$	**Arousal**	F(1,46)=0.26; p=0.614; ges=0.003	**F(2,92)=45.73; p<0.001 ges=0.307**	F(2,92)=0.67; p=0.515; ges=0.006	**t(20)=-8.22; p<0.001; d=-1.79**	**t(20)=4.67; p<0.001; d=1.02**	**t(26)=-5.34; p<0.001; d=-1.03**	**t(26)=5.34; p<0.001; d=1.03**
	Valence	F(1,46)=0.03; p=0.867; ges<0.001	**F(2,92)=53.72; p<0.001; ges=0.420**	F(2,92)=0.06; p=0.940; ges<0.001	**t(20)=-6.44; p<0.001; d=-1.40**	**t(20)=6.17; p<0.001; d=1.35**	**t(26)=-5.65; p<0.001; d=-1.09**	**t(26)=7.54; p<0.001; d=1.45**
	Contingency	F(1,46)=0.15; p=0.702; ges=0.001	**F(2,92)=44.86; p<0.001; ges=0.364**	F(2,92)=0.32; p=0.729; ges=0.004	**t(20)=-3.66; p=0.005; d=-0.799**	**t(20)=4.97; p<0.001; d=1.08**	**t(26)=-5.17; p<0.001; d=-0.995**	**t(26)=7.14; p<0.001; d=1.37**
	Reaction time	F(1,46)=2.39; p=0.129; ges=0.045	**F(1.76,81.16)=7.53; p=0.002; ges=0.014**	F(1.76,81.16)=0.89; p=0.404; ges=0.002	t(20)=-1.52; p=0.429; d=-0.332	t(20)=0.811; p=1.000; d=0.177	**t(26)=-3.23; p=0.010; d=-0.621**	t(26)=0.889; p=1.000; d=0.171

Supplementary table 2 Analyses of variances and posthoc-tests for perceived arousal, valence and contingency and reaction times to DS_{money} and $DS_{pain\ relief}$ in patients with persistent SABP and recovered SABP. Related to STAR Methods. The table shows results for analyses of variances and Bonferroni-corrected posthoc tests. All results that survived the corrected statistical threshold ($p_{bonf} < 0.05$) are depicted in bold. Abbreviations: DS: discriminative stimulus; SABP: subacute back pain; df: degrees of freedom; ges: generalized eta squared; d: Cohen's d; HAB: habitation phase; ACQ: acquisition phase; EXT: extinction phase;

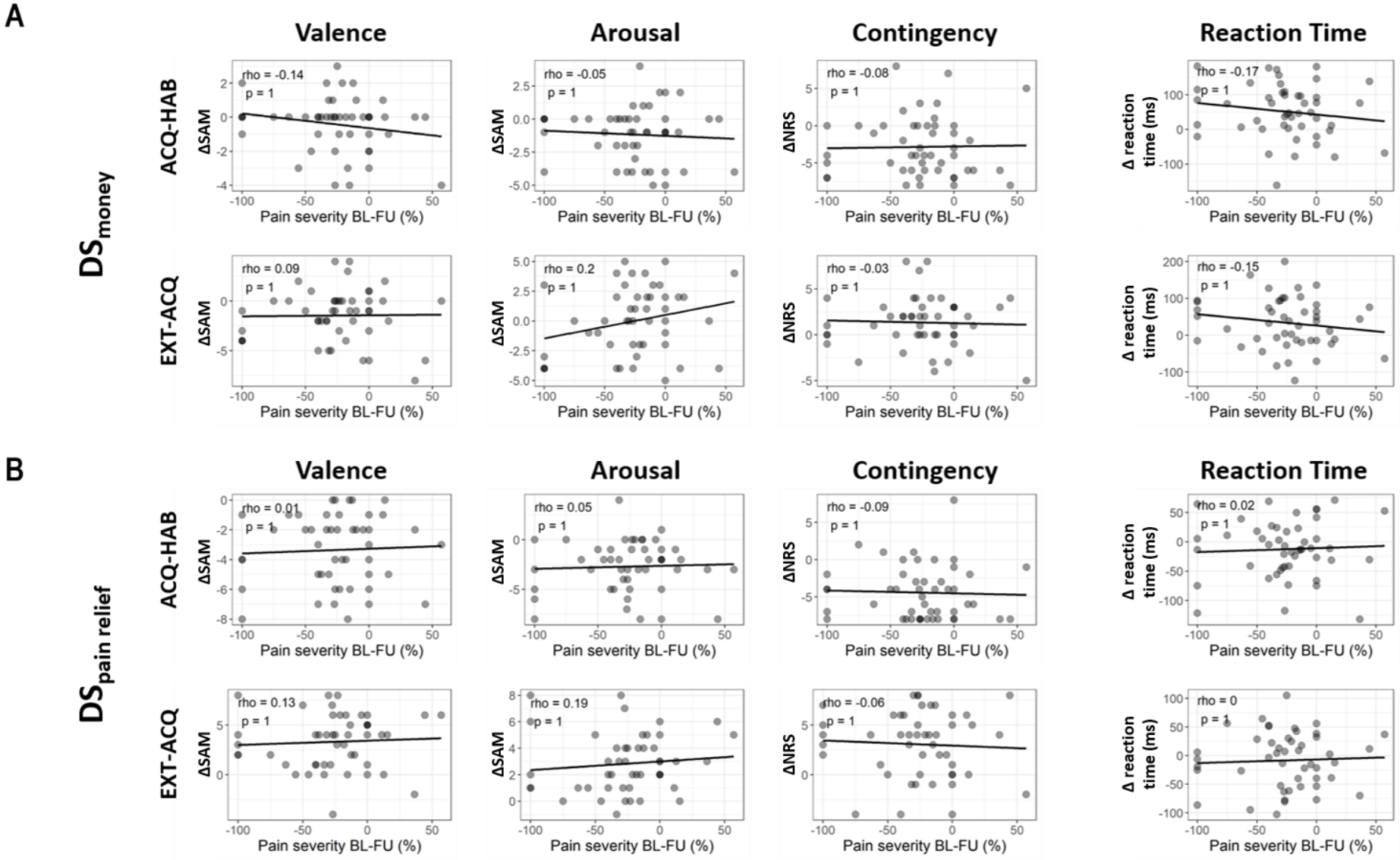
A
Valence
Arousal
Contingency
Reaction Time
DS money
ACQ-HAB
EXT-ACQ
ΔSAM
ΔNRS
Δ reaction time (ms)
Pain severity BL-FU (%)
rho = -0.14
p = 1
rho = -0.05
p = 1
rho = -0.08
p = 1
rho = -0.17
p = 1
rho = 0.09
p = 1
rho = 0.2
p = 1
rho = -0.03
p = 1
rho = -0.15
p = 1
B
DS pain relief
rho = 0.01
p = 1
rho = 0.05
p = 1
rho = -0.09
p = 1
rho = 0.02
p = 1
rho = 0.13
p = 1
rho = 0.19
p = 1
rho = -0.06
p = 1
rho = 0
p = 1

Supplementary Figure 2: learning-related changes in perceived valence, arousal and contingency of the discriminative stimuli, as well as learning-related changes in reaction time to the discriminative stimuli do not predict the transition from subacute to chronic back pain. Related to STAR Methods. *Scatter plots and spearman correlation coefficients are depicted for the change in perceived valence (first column), perceived arousal (second column), contingency (third column) and the change in reaction time (fourth column, measured in milliseconds) for* ***A)*** *the discriminative stimulus of the monetary reward condition (DS_{money}) and* ***B)*** *the discriminative stimulus of the pain relief condition. The upper row depicts the difference between the habituation and acquisition phase (acquisition minus habituation), the lower row depicts the difference between the acquisition and extinction phase (extinction minus acquisition). Correlation coefficients are shown as Spearman's Rho and reported with Bonferroni-corrected p-values (corrected for 16 tests, yielding an uncorrected threshold of $p < 0.003125$). Abbreviations: DS: discriminative stimulus; BL: baseline; FU: follow-up; HAB: habituation; ACQ: acquisition; EXT: extinction; SAM: Self-Assessment Manikin; NRS: Numeric Rating Scale; ms: milliseconds;*

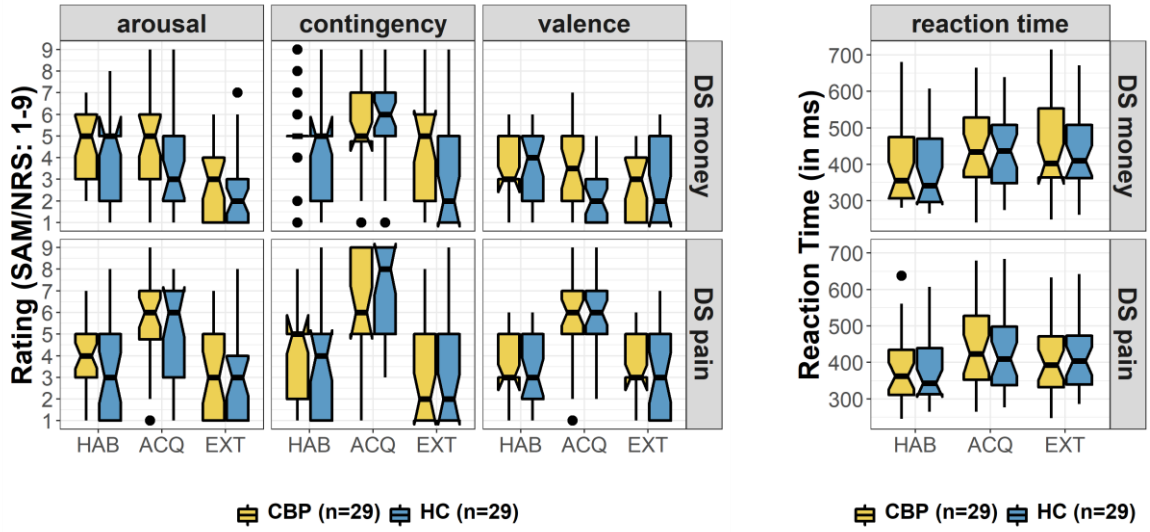

Supplementary Figure 3 depicts perceived valence, arousal and contingency of the discriminative stimuli, as well reaction time to the discriminative stimuli in patients with chronic back pain and controls. Related to STAR Methods. *Boxplots show patients with chronic back pain (CBP, yellow) and controls (HC, blue). Ratings of valence and arousal were assessed on a scale from 1 to 9 using the self-assessment manikins. Abbreviations: DS: discriminative stimulus; HAB: habituation; ACQ: acquisition; EXT: extinction; SAM: Self-Assessment Manikin; NRS: Numeric Rating Scale; ms: milliseconds;*

Analyses of perceived arousal, valence and contingency and reaction times to DS_{money} and $DS_{pain\ relief}$ in patients with persistent CBP and healthy controls

		F-Tests			Posthoc-tests: CBP		Posthoc-tests: HC	
		Group (CBP – HC): F(df); p; ges	**Phase (HAB-ACQ-EXT): F(df); p; ges**	**Group x Phase F(df); p; ges**	**HAB-ACQ t(df); p; d**	**ACQ-EXT t(df); p; d**	**HAB-ACQ t(df); p; d**	**ACQ-EXT t(df); p; d**
DS_{money}	**Arousal**	F(1,55)=2.85; p=0.097; ges=0.029	**F(2,110)=12.92; p<0.001; ges=0.091**	F(2,110)=0.43; p=0.65; ges=0.003	t(51.7)=0.72; p=1.00; d=0.193	**t(51.2)=2.83; p=0.02; d=0.752**	t(55.2)=0.12; p=1.00; d=0.032	t(53.7)=1.86; p=0.20; d=0.490
	Valence	F(1,55)=1.04; p=0.312; ges=0.011	**F(2,110)=4.44; p=0.014; ges=0.033**	F(2,110)=1.53; p=0.221; ges=0.012	t(54.5)=0.34; p=1.000; d=0.090	t(50.8)=1.40; p=0.507; d=0.371	t(54.6)=2.00; p=0.150; d=0.526	t(54.8)=-0.48; p=1.000; d=-0.127
	Contingency	F(1,55)=1.07; p=0.306; ges=0.012	**F(1.79,98.49)=17.99; p<0.001; ges=0.112**	F(1.79,98.49)=1.96; p=0.151; ges=0.014	t(54.1)=-1.09; p=0.843; d=-0-289	t(53.2)=2.02; p=0.144; d=0.535	**t(56.0)=-2.54; p=0.041; d=-0.668**	**t(55.0)=4.24; p<0.001; d=1.110**
	Reaction time	F(1,55)=0.32; p=0.577; ges=0.005	**F(1.63,89.56)=23.47; p<0.001; ges=0.043**	F(1.63,89.56)=0.95; p=0.376; ges=0.002	t(54.8)=-1.50; p=0.414; d=-0.399	t(54.8)=0.24; p=1.000; d=0.062	t(55.1)=-2.05; p=0.136; d=-0.538	t(56.0)=-0.20; p=1.000; d=-0.054
$DS_{pain\ relief}$	**Arousal**	F(1,55)=2.67; p=0.108; ges=0.025	**F(2,110)=32.91; p<0.001; ges=0.218**	F(2,110)=0.49; p=0.612; ges=0.004	**t(51.3)=-3.34; p=0.005; d=-0.886**	**t(54.6)=4.72; p<0.001; d=1.250**	**t(56.0)=-3.96; p<0.001; d=-1.040**	**t(56.0)=4.16; p<0.001; d=1.090**
	Valence	F(1,55)=0.05; p=0821.; ges<0.001	**F(1.61,88.63)=47.69; p<0.001; ges=0.341**	F(1.61,88.63)=0.24; p=0.736; ges=0.003	**t(48.1)=-4.90; p<0.001; d=-1.300**	**t(48.4)=5.24; p<0.001; d=1.390**	**t(56.0)=-6.19; p<0.001; d=-1.630**	**t(55.0)=6.04; p<0.001; d=1.590**
	Contingency	F(1,55)=0.42; p=0.518; ges=0.003	**F(1.76,96.93)=53.64; p<0.001; ges=0.372**	F(1.76,96.93)=1.65; p=0.200; ges=0.018	**t(50.2)=-3.79; p=0.001; d=-1.011**	**t(51.8)=5.86; p<0.001; d=1.560**	**t(55.2)=-6.99; p<0.001; d=-1.840**	**t(50.3)=6.92; p<0.001; d=1.820**
	Reaction time	F(1,55)=0.11; p=0.747; ges=0.002	**F(1.68,92.62)=27.08; p<0.001; ges=0.034**	F(1.68,92.62)=0.48; p=0.588; ges<0.001	t(54.7)=-1.61; p=0.342; d=-0.426	t(54.6)=0.58; p=1.000; d=0.153	t(54.0)=-1.76; p=0.253; d=-0.462	t(55.7)=0.21; p=1.000; d=0.055

Supplementary table 3 Analyses of variances and posthoc-tests for perceived arousal, valence and contingency and reaction times to DS_{money} and $DS_{pain\ relief}$ in patients with CBP and HC. Related to STAR Methods. The table shows results for analyses of variances and Bonferroni-corrected posthoc tests. All results that survived the corrected statistical threshold ($p_{bonf} < 0.05$) are depicted in bold. Abbreviations: DS: discriminative stimulus; HC: healthy controls; CBP: chronic back pain; df: degrees of freedom; ges: generalized eta squared; d: Cohen's d; HAB: habituation phase; ACQ: acquisition phase; EXT: extinction phase;

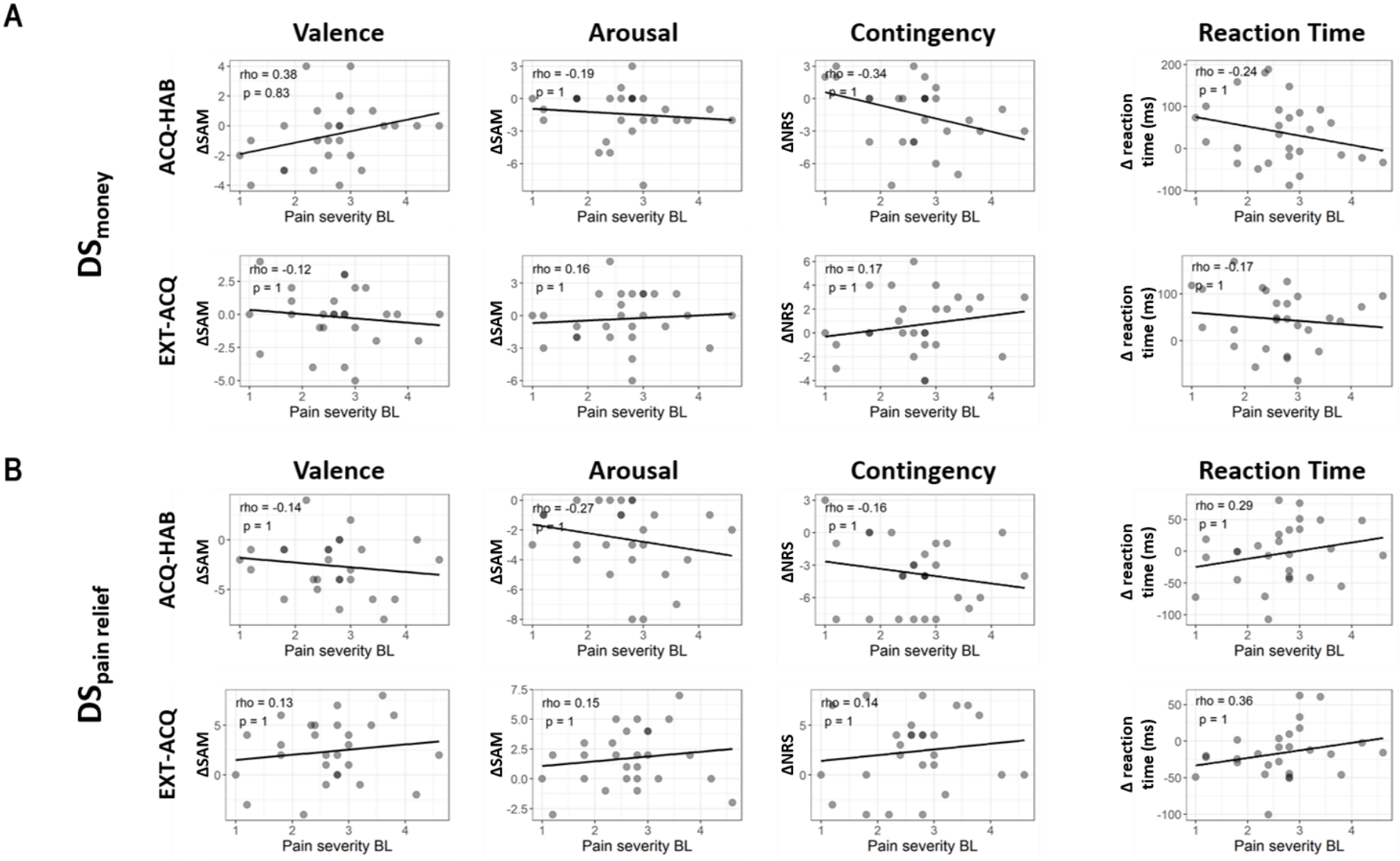
A
Valence
Arousal
Contingency
Reaction Time
DS money
ACQ-HAB
EXT-ACQ
ΔSAM
ΔNRS
Δ reaction time (ms)
Pain severity BL
rho = 0.38
p = 0.83
rho = -0.19
p = 1
rho = -0.34
p = 1
rho = -0.24
p = 1
rho = -0.12
p = 1
rho = 0.16
p = 1
rho = 0.17
p = 1
rho = -0.17
p = 1
B
Valence
Arousal
Contingency
Reaction Time
DS pain relief
ACQ-HAB
EXT-ACQ
ΔSAM
ΔNRS
Δ reaction time (ms)
Pain severity BL
rho = -0.14
p = 1
rho = -0.27
p = 1
rho = -0.16
p = 1
rho = 0.29
p = 1
rho = 0.13
p = 1
rho = 0.15
p = 1
rho = 0.14
p = 1
rho = 0.36
p = 1

Supplementary Figure 4: Learning-related changes in perceived valence, arousal and contingency of the discriminative stimuli, as well as learning-related changes in reaction time to the discriminative stimuli are not related to severity of chronic back pain. Related to STAR Methods. Scatter plots and spearman correlation coefficients are depicted for the change in perceived valence (first column), perceived arousal (second column), contingency (third column) and the change in reaction time (fourth column, measured in milliseconds) for ***A)*** *the discriminative stimulus of the monetary reward condition (DS_{money}) and* ***B)*** *the discriminative stimulus of the pain relief condition. The upper row depicts the difference between the habituation and acquisition phase (acquisition minus habituation), the lower row depicts the difference between the acquisition and extinction phase (extinction minus acquisition). Correlation coefficients are shown as Spearman's Rho and reported with Bonferroni-corrected p-values (corrected for 16 tests, yielding an uncorrected threshold of $p < 0.003125$). Abbreviations: DS: discriminative stimulus; BL: baseline; HAB: habituation; ACQ: acquisition; EXT: extinction; SAM: Self-Assessment Manikin; NRS: Numeric Rating Scale; ms: milliseconds;*

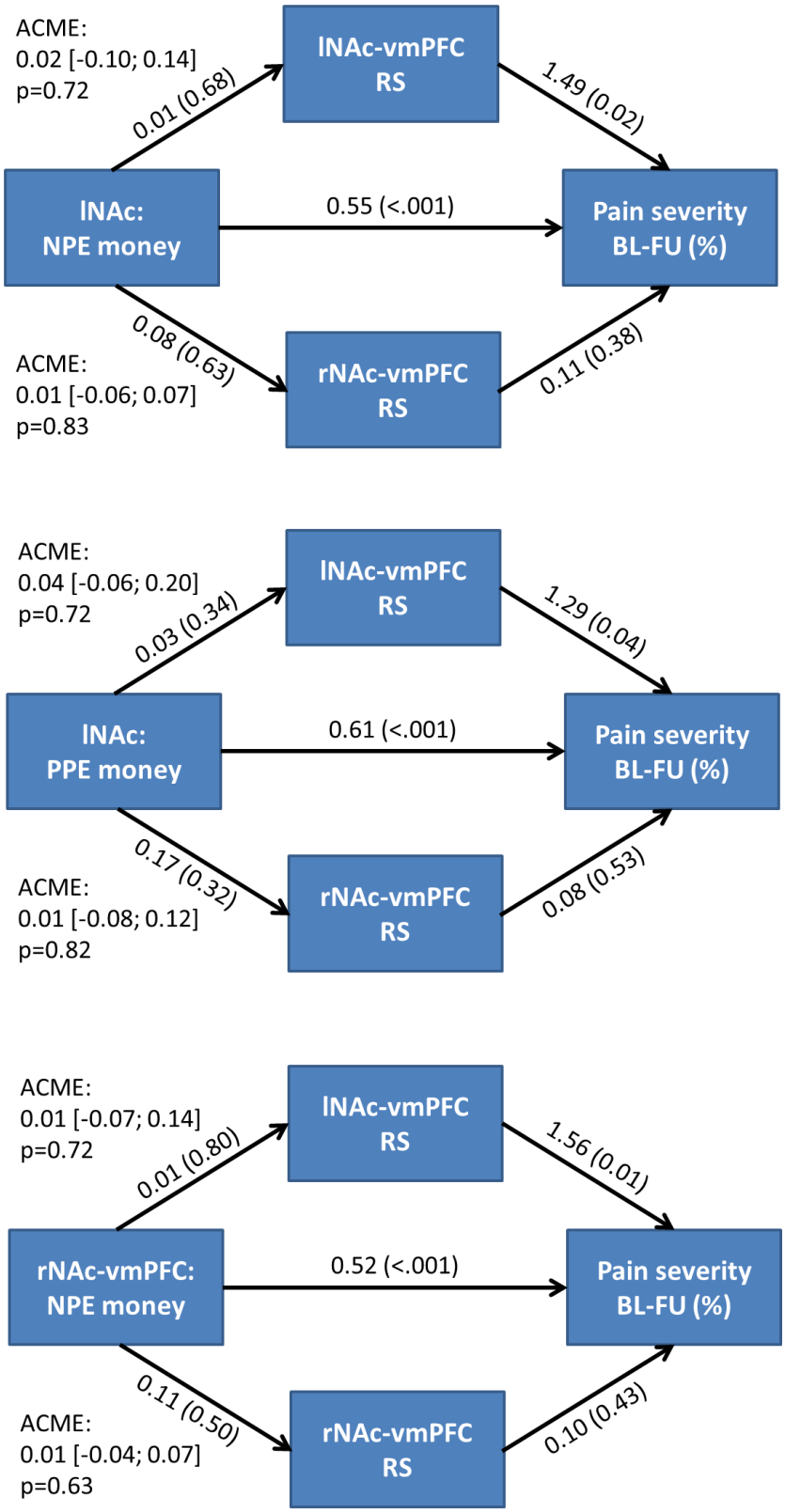

Supplementary Figure 5: Task-based prediction of chronicity was not mediated via functional connectivity of nucleus accumbens and ventromedial prefrontal cortex at rest shows. Related to Figures 2 and 3. The graphs depict results of mediation analysis with functional connectivity between vmPFC and left NAc (upper branch of the models) and right NAc (lower branch of the models) as mediating variable, encoding of monetary prediction error as independent and percentage change in pain severity from baseline to follow-up as dependent variable. Coefficients are given with p-values in round brackets in addition to the average causal mediation effect with 95 percent confidence intervals in square brackets for each model. Abbreviations: vmPFC: ventromedial prefrontal cortex; lNAc: left nucleus accumbens; rNAc: right nucleus accumbens; BL: baseline; FU: follow-up; RS: resting state; NPE: negative prediction error; PPE: positive prediction error; ACME: average causal mediation effect;

Correlation of BOLD responses in vmPFC and NAc with percent change in pain severity from baseline to follow-up				
	ROI	**Contrast**	**Pearson's correlation: r(df); p, p_{bonf}**	**ROC: Area under curve**
Parameter estimate of BOLD contrast	Left nucleus accumbens	Anticipation money	r(46)=0.07; p=0.632; pbonf=1	AUC=0.53; p=0.379; pbonf=1
		Anticipation pain relief	r(46)=-0.06; p=0.661; pbonf=1	AUC=0.44; p=0.758; pbonf=1
		DS money	r(46)=-0.34; p=0.018; pbonf=0.827	AUC=0.29; p=0.995; pbonf=1
		DS pain	r(46)=-0.17; p=0.235; pbonf=1	AUC=0.31; p=0.989; pbonf=1
		Positive prediction error: money	**r(46)=0.61; p<0.001; pbonf<0.001**	**AUC=0.77; p<0.001; pbonf=0.021**
		Negative prediction error: money	**r(46)=0.55; p<0.001; pbonf=0.002**	**AUC=0.83; p<0.001; pbonf<0.001**
		Positive prediction error: pain relief	r(46)=0.18; p=0.212; pbonf=1	AUC=0.63; p=0.068; pbonf=1
		Negative prediction error: pain relief	r(46)=0.12; p=0.416; pbonf=1	AUC=0.61; p=0.096; pbonf=1
		US pain	r(46)=0.36; p=0.012; pbonf=0.558	AUC=0.68; p=0.018; pbonf=0.806
	Right nucleus accumbens	Anticipation money	r(46)=0.08; p=0.598; pbonf=1	AUC=0.52; p=0.418; pbonf=1
		Anticipation pain relief	r(46)=0.07; p=0.628; pbonf=1	AUC=0.53; p=0.387; pbonf=1
		DS money	r(46)=0.00; p=0.999; pbonf=1	AUC=0.53; p=0.348; pbonf=1
		DS pain	r(46)=0.26; p=0.076; pbonf=1	AUC=0.56; p=0.261; pbonf=1
		Positive prediction error: money	r(46)=0.08; p=0.583; pbonf=1	AUC=0.53; p=0.379; pbonf=1
		Negative prediction error: money	r(46)=0.00; p=0.998; pbonf=1	AUC=0.48; p=0.590; pbonf=1
		Positive prediction error: pain relief	r(46)=-0.08; p=0.606; pbonf=1	AUC=0.48; p=0.598; pbonf=1
		Negative prediction error: pain relief	r(46)=-0.06; p=0.692; pbonf=1	AUC=0.49; p=0.565; pbonf=1
		US pain	r(46)=-0.11; p=0.445; pbonf=1	AUC=0.50; p=0.508; pbonf=1
	vmPFC	Anticipation money	r(46)=0.04; p=0.812; pbonf=1	AUC=0.41; p=0.849; pbonf=1
		Anticipation pain relief	r(46)=-0.06; p=0.670; pbonf=1	AUC=0.40; p=0.893; pbonf=1
		DS money	r(46)=0.25; p=0.089; pbonf=1	AUC=0.56; p=0.248; pbonf=1
		DS pain	r(46)=0.13; p=0.376; pbonf=1	AUC=0.41; p=0.849; pbonf=1
		Positive prediction error: money	r(46)=-0.10; p=0.518; pbonf=1	AUC=0.41; p=0.863; pbonf=1
		Negative prediction error: money	r(46)=-0.12; p=0.412; pbonf=1	AUC=0.44; p=0.758; pbonf=1
		Positive prediction error: pain relief	r(46)=0.10; p=0.502; pbonf=1	AUC=0.65; p=0.042; pbonf=1
		Negative prediction error: pain relief	r(46)=0.09; p=0.538; pbonf=1	AUC=0.66; p=0.029; pbonf=1
		US pain	r(46)=0.04; p=0.809; pbonf=1	AUC=0.48; p=0.582; pbonf=1

Supplementary table 4 Prediction of transition from subacute to chronic back pain with responses to different reward learning processes in the nucleus accumbens and ventromedial prefrontal cortex (vmPFC), related to Figure 2. The table shows correlations between the percentage change in pain severity from baseline to the six month follow-up and the BOLD response to different learning processes in the respective region. BOLD responses were extracted as parameter estimates from predefined masks extracted from neurosynth.org (see above). Correlations are reported as Pearson's correlation with degrees of freedom (df), uncorrected p-values and Bonferroni-corrected p-values (corrected for 45 tests yielding, a threshold of p < 0.00111). Additionally we divided patients in recovered patients if their pain severity decreased by 20% between the first

examination and the follow-up assessment patients and persistent patients in all other instances. Receiver operating characteristic (ROC) curves were created for classifying recovered and persistent patients with the respective parameter estimates extracted from our regions of interest. We report the area under each ROC curves as an estimate of sensitivity and specificity. Associated p-values for the comparison to a chance-level ROC curve (i.e. AUC = 0.5) are reported as uncorrected p-values as well as Bonferroni-corrected p-values (corrected for 45 tests, yielding a threshold of $p < 0.00111$). All results that survived the corrected statistical significant ($p_{bonf} < 0.05$) are depicted in bold.

Correlation of functional connectivity with the vmPFC and the percent change in pain severity from baseline to follow-up				
	ROI	**Contrast**	**Pearson's correlation: r(df); p, p_{bonf}**	**ROC: Area under curve**
Functional connectivity with vmPFC	Left nucleus accumbens	Anticipation money	r(46)=0.00; p=0.982; pbonf=1	AUC=0.64; p=0.055; pbonf=1
		Anticipation pain relief	r(46)=0.05; p=0.739; pbonf=1	AUC=0.52; p=0.402; pbonf=1
		DS money	r(46)=-0.11; p=0.441; pbonf=1	AUC=0.51; p=0.475; pbonf=1
		DS pain	r(46)=-0.41; p=0.004; pbonf=0.165	AUC=0.39; p=0.907; pbonf=1
		Positive prediction error: money	r(46)=0.16; p=0.265; pbonf=1	AUC=0.57; p=0.217; pbonf=1
		Negative prediction error: money	r(46)=0.12; p=0.411; pbonf=1	AUC=0.64; p=0.055; pbonf=1
		Positive prediction error: pain relief	r(46)=0.01; p=0.948; pbonf=1	AUC=0.49; p=0.565; pbonf=1
		Negative prediction error: pain relief	r(46)=-0.04; p=0.786; pbonf=1	AUC=0.50; p=0.500; pbonf=1
		US pain	r(46)=-0.11; p=0.459; pbonf=1	AUC=0.46; p=0.704; pbonf=1
	Right nucleus accumbens	Anticipation money	r(46)=0.20; p=0.167; pbonf=1	AUC=0.53; p=0.379; pbonf=1
		Anticipation pain relief	r(46)=0.00; p=0.986; pbonf=1	AUC=0.53; p=0.363; pbonf=1
		DS money	r(46)=0.07; p=0.631; pbonf=1	AUC=0.54; p=0.340; pbonf=1
		DS pain	r(46)=0.13; p=0.372; pbonf=1	AUC=0.51; p=0.443; pbonf=1
		Positive prediction error: money	r(46)=-0.06; p=0.694; pbonf=1	AUC=0.54; p=0.340; pbonf=1
		Negative prediction error: money	**r(46)=0.52; p<0.001; pbonf=0.006**	**AUC=0.78; p<0.001; pbonf=0.021**
		Positive prediction error: pain relief	r(46)=0.14; p=0.348; pbonf=1	AUC=0.59; p=0.156; pbonf=1
		Negative prediction error: pain relief	r(46)=0.41; p=0.004; pbonf=0.191	AUC=0.66; p=0.026; pbonf=1
		US pain	r(46)=-0.13; p=0.397; pbonf=1	AUC=0.43; p=0.807; pbonf=1

Supplementary table 5 Prediction of transition from subacute to chronic back pain with task-based functional connectivity between ventromedial prefrontal cortex (vmPFC) and bilateral nucleus accumbens during different reward learning processes, related to Figure 2. The table shows correlations between the percentage change in pain severity from baseline to the six month follow-up and the task-based functional connectivity between the ventromedial prefrontal cortex and bilateral nucleus accumbens during different learning processes in the respective region. Parameter estimates were extracted from predefined masks extracted from neurosynth.org (see above), using a psychophysiological interaction (PPI) with the vmPFC as a seed region. Correlations are reported as Pearson's correlation with degrees of freedom (df), uncorrected p-values and Bonferroni-corrected p-values (corrected for 45 tests, yielding a threshold of p < 0.00111). Additionally we divided patients in recovered patients if their pain severity decreased by 20% between the first examination and the follow-up assessment patients and persistent patients in all other instances. Receiver operating characteristic (ROC) curves were created for classifying recovered and persistent patients with the respective parameter estimates extracted from our regions of interest. We report the area under each ROC curves as an estimate of sensitivity and specificity. Associated p-values for the comparison to a chance-level ROC curve (i.e. AUC = 0.5) are reported as uncorrected p-values as well as Bonferroni-corrected p-values (corrected for 45 tests, yielding a threshold of p < 0.00111). All results that survived the corrected statistical threshold (p_{bonf} < 0.05) are depicted in bold.

Correlation of BOLD responses in vmPFC and NAc during habituation and extinction with percent change in pain severity from baseline to follow-up

	Phase(s)	Contrast	ROI	Pearson's correlation: r(df); p, pbonf	ROC: Area under curve
Parameter estimate of BOLD contrast	Habituation	DS money	lNA	r(46)=-0.09; p=0.560; pbonf=1	AUC=0.41; p=0.868; pbonf=1
		DS money	rNA	r(46)=0.08; p=0.570; pbonf=1	AUC=0.46; p=0.675; pbonf=1
		DS money	vmPFC	r(46)=0.33; p=0.023; pbonf=0.558	AUC=0.71; p=0.007; pbonf=0.159
		DS pain	lNA	r(46)=0.19; p=0.204; pbonf=1	AUC=0.60; p=0.128; pbonf=1
		DS pain	rNA	r(46)=0.12; p=0.413; pbonf=1	AUC=0.58; p=0.166; pbonf=1
		DS pain	vmPFC	r(46)=0.12; p=0.407; pbonf=1	AUC=0.66; p=0.026; pbonf=0.632
	Habituation < Acquisition	DS money	lNA	r(46)=-0.05; p=0.719; pbonf=1	AUC=0.51; p=0.451; pbonf=1
		DS money	rNA	r(46)=-0.08; p=0.602; pbonf=1	AUC=0.44; p=0.771; pbonf=1
		DS money	vmPFC	r(46)=0.12; p=0.435; pbonf=1	AUC=0.61; p=0.103; pbonf=1
		DS pain	lNA	r(46)=0.25; p=0.081; pbonf=1	AUC=0.66; p=0.032; pbonf=0.768
		DS pain	rNA	r(46)=0.15; p=0.322; pbonf=1	AUC=0.61; p=0.096; pbonf=1
		DS pain	vmPFC	r(46)=0.17; p=0.241; pbonf=1	AUC=0.72; p=0.005; pbonf=0.116
	Extinction	DS money	lNA	r(46)=-0.06; p=0.697; pbonf=1	AUC=0.47; p=0.637; pbonf=1
		DS money	rNA	r(46)=-0.03; p=0.836; pbonf=1	AUC=0.47; p=0.629; pbonf=1
		DS money	vmPFC	r(46)=0.10; p=0.496; pbonf=1	AUC=0.54; p=0.340; pbonf=1
		DS pain	lNA	r(46)=0.03; p=0.849; pbonf=1	AUC=0.46; p=0.697; pbonf=1
		DS pain	rNA	r(46)=-0.02; p=0.914; pbonf=1	AUC=0.49; p=0.557; pbonf=1
		DS pain	vmPFC	r(46)=0.16; p=0.288; pbonf=1	AUC=0.54; p=0.311; pbonf=1
	Acquistion > Extinction	DS money	lNA	r(46)=0.07; p=0.620; pbonf=1	AUC=0.55; p=0.296; pbonf=1
		DS money	rNA	r(46)=-0.01; p=0.922; pbonf=1	AUC=0.54; p=0.311; pbonf=1
		DS money	vmPFC	r(46)=-0.20; p=0.180; pbonf=1	AUC=0.37; p=0.935; pbonf=1
		DS pain	lNA	r(46)=-0.27; p=0.066; pbonf=1	AUC=0.37; p=0.943; pbonf=1
		DS pain	rNA	r(46)=-0.16; p=0.268; pbonf=1	AUC=0.39; p=0.904; pbonf=1
		DS pain	vmPFC	r(46)=-0.18; p=0.228; pbonf=1	AUC=0.27; p=0.997; pbonf=1

Supplementary table 6: Prediction of transition from subacute to chronic back pain with responses to discriminative stimuli (DS) during habituation, extinction and changes from habituation to acquisition and acquisition to extinction in the nucleus accumbens and ventromedial prefrontal cortex (vmPFC). Related to STAR Methods. The table shows correlations between the percentage change in pain severity from baseline to the six month follow-up and the BOLD response to different learning processes in the respective region. BOLD responses were extracted as parameter estimates from predefined masks extracted from neurosynth.org. Correlations are reported as Pearson's correlation with degrees of freedom (df), uncorrected p-values and Bonferroni-corrected p-values (corrected for 24 tests yielding, a threshold of $p < 0.00208$). Additionally we divided patients in recovered patients if their pain severity decreased by 20% between the first examination and the follow-up assessment patients and persistent patients in all other instances. Receiver operating characteristic (ROC) curves were created for classifying recovered and persistent patients with the respective parameter estimates extracted from our regions of interest. We report the area under each ROC curves as an estimate of sensitivity and specificity. Associated p-values for the comparison to a chance-level ROC curve (i.e. AUC = 0.5) are reported as uncorrected p-values as well as Bonferroni-corrected p-values (corrected for 24 tests, yielding a threshold of $p < 0.00208$).

Prediction of chronicity with patterns of BOLD responses in vmPFC and NAc					
			Accuracy M±SD	**One-sample t-test (against Accuracy = 0.5): t(df); p; pbonf; d**	**ROC: Area under curve**
Pattern of BOLD contrast	Left nucleus accumbens	Anticipation money	0.48±0.39	t(47)=-0.40; p=0.69; pbonf=1; d=0.06	AUC=0.49; p=0.55; pbonf=1
		Anticipation pain relief	0.49±0.39	t(47)=-0.15; p=0.88; pbonf=1; d=0.02	AUC=0.49; p=0.57; pbonf=1
		DS money	0.52±0.39	t(47)=0.30; p=0.76; pbonf=1; d=0.04	AUC=0.51; p=0.46; pbonf=1
		DS pain	0.44±0.38	t(47)=-1.10; p=0.28; pbonf=1; d=0.16	AUC=0.43; p=0.81; pbonf=1
		Positive prediction error: money	0.47±0.39	t(47)=-0.54; p=0.59; pbonf=1; d=0.08	AUC=0.49; p=0.56; pbonf=1
		Negative prediction error: money	0.62±0.40	t(47)=2.09; p=0.04; pbonf=1; d=0.30	AUC=0.68; p=0.02; pbonf=0.85
		Positive prediction error: pain relief	0.44±0.37	t(47)=-1.08; p=0.29; pbonf=1; d=0.16	AUC=0.40; p=0.88; pbonf=1
		Negative prediction error: pain relief	0.44±0.37	t(47)=-1.03; p=0.31; pbonf=1; d=0.15	AUC=0.40; p=0.88; pbonf=1
		US pain	0.46±0.38	t(47)=-0.66; p=0.51; pbonf=1; d=0.10	AUC=0.40; p=0.89; pbonf=1
	Right nucleus accumbens	Anticipation money	0.40±0.36	t(47)=-1.88; p=0.07; pbonf=1; d=0.27	AUC=0.34; p=0.97; pbonf=1
		Anticipation pain relief	0.55±0.39	t(47)=0.91; p=0.37; pbonf=1; d=0.13	AUC=0.59; p=0.16; pbonf=1
		DS money	0.42±0.36	t(47)=-1.60; p=0.12; pbonf=1; d=0.23	AUC=0.38; p=0.92; pbonf=1
		DS pain	**0.71±0.34**	**t(47)=4.30; p<0.001; pbonf=0.004; d=0.62**	**AUC=0.8; p<0.001; pbonf=0.009**
		Positive prediction error: money	0.55±0.38	t(47)=0.84; p=0.40; pbonf=1; d=0.12	AUC=0.57; p=0.20; pbonf=1
		Negative prediction error: money	0.55±0.42	t(47)=0.81; p=0.42; pbonf=1; d=0.12	AUC=0.56; p=0.24; pbonf=1
		Positive prediction error: pain relief	0.53±0.40	t(47)=0.47; p=0.64; pbonf=1; d=0.07	AUC=0.56; p=0.25; pbonf=1
		Negative prediction error: pain relief	0.54±0.40	t(47)=0.65; p=0.52; pbonf=1; d=0.09	AUC=0.56; p=0.25; pbonf=1
		US pain	0.57±0.42	t(47)=1.18; p=0.24; pbonf=1; d=0.17	AUC=0.59; p=0.13; pbonf=1
	vmPFC	Anticipation money	0.40±0.40	t(47)=-1.81; p=0.08; pbonf=1; d=0.26	AUC=0.33; p=0.98; pbonf=1
		Anticipation pain relief	0.40±0.39	t(47)=-1.76; p=0.08; pbonf=1; d=0.25	AUC=0.35; p=0.97; pbonf=1
		DS money	0.57±0.40	t(47)=1.22; p=0.23; pbonf=1; d=0.18	AUC=0.59; p=0.13; pbonf=1
		DS pain	0.36±0.39	t(47)=-2.48; p=0.02; pbonf=0.75; d=0.36	AUC=0.31; p=0.99; pbonf=1
		Positive prediction error: money	0.41±0.41	t(47)=-1.47; p=0.15; pbonf=1; d=0.21	AUC=0.41; p=0.86; pbonf=1
		Negative prediction error: money	0.37±0.40	t(47)=-2.23; p=0.03; pbonf=1; d=0.32	AUC=0.33; p=0.98; pbonf=1
		Positive prediction error: pain relief	0.41±0.36	t(47)=-1.66; p=0.10; pbonf=1; d=0.24	AUC=0.34; p=0.97; pbonf=1
		Negative prediction error: pain relief	0.42±0.36	t(47)=-1.57; p=0.12; pbonf=1; d=0.23	AUC=0.36; p=0.96; pbonf=1
		US pain	0.60±0.41	t(47)=1.62; p=0.11; pbonf=1; d=0.23	AUC=0.63; p=0.05; pbonf=1

Supplementary table 7 Prediction of transition from subacute to chronic back pain with patterns of activation in the nucleus accumbens and ventromedial prefrontal cortex (vmPFC) in response to different reward learning processes, related to Figure 4. The table shows how good of patterns of activity in response to different reward learning processes classify recovered and non-recovered persons. Mean accuracy across subjects is reported and tested against chance level accuracy (50%) using a one-sample t-test with degrees of freedom (df), uncorrected p-values and Bonferroni-corrected p-values (corrected for 45 tests yielding an uncorrected threshold of p < 0.00111) and Cohen's d.

Additionally receiver operating characteristic (ROC) curves were created for correctly classifying persistent patients with the respective pattern of activity. We report the area under each ROC curves as an estimate of sensitivity and specificity. Associated p-values for the comparison to a chance-level ROC curve (i.e. AUC = 0.5) are reported as uncorrected p-values as well as Bonferroni-corrected p-values (corrected for 45 tests yielding an uncorrected threshold of $p < 0.00111$).). All results that survived the corrected statistical threshold ($p_{bonf} < 0.05$) are depicted in bold.

Prediction of chronicity with patterns of functional connectivity to the vmPFC					
			Accuracy M±SD	**One-sample t-test (against Accuracy = 0.5): t(df); p; pbonf; d**	**ROC: Area under curve**
Pattern of functional connectivity to the vmPFC	Left nucleus accumbens	Anticipation money	0.54±0.35	t(47)=0.75; p=0.46; pbonf=1; d=0.11	AUC=0.58; p=0.19; pbonf=1
		Anticipation pain relief	0.54±0.36	t(47)=0.77; p=0.44; pbonf=1; d=0.11	AUC=0.59; p=0.15; pbonf=1
		DS money	0.44±0.33	t(47)=-1.19; p=0.24; pbonf=1; d=0.17	AUC=0.41; p=0.86; pbonf=1
		DS pain	0.53±0.36	t(47)=0.54; p=0.59; pbonf=1; d=0.08	AUC=0.56; p=0.25; pbonf=1
		Positive prediction error: money	0.54±0.38	t(47)=0.67; p=0.51; pbonf=1; d=0.10	AUC=0.56; p=0.25; pbonf=1
		Negative prediction error: money	0.49±0.36	t(47)=-0.26; p=0.80; pbonf=1; d=0.04	AUC=0.46; p=0.67; pbonf=1
		Positive prediction error: pain relief	0.64±0.34	t(47)=2.88; p=0.01; pbonf=0.27; d=0.42	AUC=0.73; p=0.003; pbonf=0.15
		Negative prediction error: pain relief	0.42±0.36	t(47)=-1.55; p=0.13; pbonf=1; d=0.22	AUC=0.38; p=0.93; pbonf=1
		US pain	0.52±0.34	t(47)=0.34; p=0.74; pbonf=1; d=0.05	AUC=0.52; p=0.41; pbonf=1
	Right nucleus accumbens	Anticipation money	0.41±0.37	t(47)=-1.61; p=0.11; pbonf=1; d=0.23	AUC=0.36; p=0.95; pbonf=1
		Anticipation pain relief	0.56±0.36	t(47)=1.17; p=0.25; pbonf=1; d=0.17	AUC=0.59; p=0.15; pbonf=1
		DS money	0.44±0.35	t(47)=-1.23; p=0.23; pbonf=1; d=0.18	AUC=0.42; p=0.83; pbonf=1
		DS pain	0.65±0.33	t(47)=3.16; p=0.003; pbonf=0.123; d=0.46	AUC=0.74; p=0.002; pbonf=0.101
		Positive prediction error: money	0.58±0.36	t(47)=1.49; p=0.14; pbonf=1; d=0.21	AUC=0.62; p=0.09; pbonf=1
		Negative prediction error: money	0.52±0.36	t(47)=0.32; p=0.75; pbonf=1; d=0.05	AUC=0.52; p=0.39; pbonf=1
		Positive prediction error: pain relief	0.49±0.35	t(47)=-0.21; p=0.83; pbonf=1; d=0.03	AUC=0.50; p=0.50; pbonf=1
		Negative prediction error: pain relief	0.52±0.38	t(47)=0.28; p=0.78; pbonf=1; d=0.04	AUC=0.56; p=0.25; pbonf=1
		US pain	0.50±0.35	t(47)=0.06; p=0.95; pbonf=1; d=0.01	AUC=0.49; p=0.53; pbonf=1

Supplementary table 8: Prediction of transition from subacute to chronic back pain with patterns of functional connectivity between the nucleus accumbens and ventromedial prefrontal cortex (vmPFC) in response to different reward learning processes. Related to STAR Methods. The table shows how good patterns of functional connectivity to the vmPFC in response to different reward learning processes classify recovered and non-recovered persons. Mean accuracy across subjects is reported and tested against chance level accuracy (50%) using a one-sample t-test with degrees of freedom (df), uncorrected p-values and Bonferroni-corrected p-values (corrected for 45 tests yielding an uncorrected threshold of p < 0.00111) and Cohen's d. Additionally receiver operating characteristic (ROC) curves were created for correctly classifying persistent patients with the respective pattern of connectivity. We report the area under each ROC curve as an estimate of sensitivity and specificity. Associated p-values for the comparison to a chance-level ROC curve (i.e. AUC = 0.5) are reported as uncorrected p-values as well as Bonferroni-corrected p-values (corrected for 45 tests yielding an uncorrected threshold of p < 0.00111).

BOLD responses in vmPFC and NAc: correlation with pain severity in patients with CBP and dissociation between CBP and HC				
	ROI	Contrast	Pearson's correlation: r(df); p, p_{bonf}	ROC: Area under curve
Parameter estimate of BOLD contrast	Left nucleus accumbens	Anticipation money	r(27)=-0.29; p=0.120; pbonf=1	AUC=0.43; p=0.819; pbonf=1
		Anticipation pain relief	r(27)=-0.24; p=0.211; pbonf=1	AUC=0.43; p=0.807; pbonf=1
		DS money	r(27)=-0.06; p=0.764; pbonf=1	AUC=0.47; p=0.633; pbonf=1
		DS pain	r(27)=-0.34; p=0.073; pbonf=1	AUC=0.43; p=0.823; pbonf=1
		Positive prediction error: money	r(27)=0.27; p=0.160; pbonf=1	AUC=0.34; p=0.985; pbonf=1
		Negative prediction error: money	r(27)=0.31; p=0.103; pbonf=1	AUC=0.44; p=0.798; pbonf=1
		Positive prediction error: pain relief	r(27)=-0.03; p=0.864; pbonf=1	AUC=0.55; p=0.273; pbonf=1
		Negative prediction error: pain relief	r(27)=-0.04; p=0.833; pbonf=1	AUC=0.53; p=0.333; pbonf=1
		US pain	r(27)=0.09; p=0.632; pbonf=1	AUC=0.58; p=0.154; pbonf=1
	Right nucleus accumbens	Anticipation money	r(27)=-0.05; p=0.800; pbonf=1	AUC=0.40; p=0.901; pbonf=1
		Anticipation pain relief	r(27)=-0.24; p=0.209; pbonf=1	AUC=0.57; p=0.173; pbonf=1
		DS money	r(27)=0.20; p=0.288; pbonf=1	AUC=0.50; p=0.518; pbonf=1
		DS pain	r(27)=-0.01; p=0.978; pbonf=1	AUC=0.37; p=0.953; pbonf=1
		Positive prediction error: money	r(27)=0.25; p=0.184; pbonf=1	AUC=0.51; p=0.457; pbonf=1
		Negative prediction error: money	r(27)=0.08; p=0.662; pbonf=1	AUC=0.55; p=0.253; pbonf=1
		Positive prediction error: pain relief	r(27)=0.12; p=0.528; pbonf=1	AUC=0.44; p=0.798; pbonf=1
		Negative prediction error: pain relief	r(27)=0.07; p=0.724; pbonf=1	AUC=0.44; p=0.794; pbonf=1
		US pain	r(27)=0.08; p=0.699; pbonf=1	AUC=0.53; p=0.373; pbonf=1
	vmPFC	Anticipation money	r(27)=-0.36; p=0.056; pbonf=1	AUC=0.46; p=0.689; pbonf=1
		Anticipation pain relief	r(27)=0.29; p=0.132; pbonf=1	AUC=0.59; p=0.126; pbonf=1
		DS money	r(27)=-0.14; p=0.480; pbonf=1	AUC=0.62; p=0.064; pbonf=1
		DS pain	r(27)=-0.21; p=0.271; pbonf=1	AUC=0.51; p=0.445; pbonf=1
		Positive prediction error: money	r(27)=-0.09; p=0.651; pbonf=1	AUC=0.36; p=0.970; pbonf=1
		Negative prediction error: money	r(27)=-0.20; p=0.301; pbonf=1	AUC=0.45; p=0.752; pbonf=1
		Positive prediction error: pain relief	r(27)=-0.30; p=0.119; pbonf=1	AUC=0.41; p=0.892; pbonf=1
		Negative prediction error: pain relief	r(27)=-0.35; p=0.063; pbonf=1	AUC=0.42; p=0.839; pbonf=1
		US pain	r(27)=-0.07; p=0.731; pbonf=1	AUC=0.54; p=0.300; pbonf=1

Supplementary table 9: fronto-striatal encoding of reward learning is not associated with pain severity in patients with chronic back pain, related to Figure 5. The table shows correlations between the pain severity of patients with chronic back pain and the BOLD response to different learning processes in the respective region. BOLD responses were extracted as parameter estimates from predefined masks extracted from neurosynth.org (see above). Correlations are reported as Pearson's correlation with degrees of freedom (df), uncorrected p-values and Bonferroni-corrected p-values (corrected for 45 tests yielding a threshold of $p < 0.00111$). Additionally we created receiver operating

characteristic (ROC) curves for classifying patients with chronic back pain and controls with the respective parameter estimates extracted from our regions of interest. We report the area under each ROC curves as an estimate of sensitivity and specificity. Associated p-values for the comparison to a chance-level ROC curve (i.e. AUC = 0.5) are reported as uncorrected p-values as well as Bonferroni-corrected p-values (corrected for 45 tests yielding a threshold of $p < 0.00111$). Al results that survived the corrected statistical threshold ($p_{bonf} < 0.05$) are depicted in bold.

Functional connectivity with vmPFC: Correlation with pain severity in patients with CBP and dissociation between CBP and HC				
ROI		**Contrast**	**Pearson's correlation: r(df); p, p_{bonf}**	**ROC: Area under curve**
Functional connectivity with vmPFC	Left nucleus accumbens	Anticipation money	r(27)=0.05; p=0.799; pbonf=1	AUC=0.44; p=0.802; pbonf=1
		Anticipation pain relief	r(27)=-0.18; p=0.361; pbonf=1	AUC=0.55; p=0.279; pbonf=1
		DS money	r(27)=0.01; p=0.976; pbonf=1	AUC=0.63; p=0.050; pbonf=1
		DS pain	r(27)=-0.11; p=0.572; pbonf=1	AUC=0.53; p=0.333; pbonf=1
		Positive prediction error: money	r(27)=-0.26; p=0.171; pbonf=1	AUC=0.61; p=0.070; pbonf=1
		Negative prediction error: money	r(27)=-0.27; p=0.154; pbonf=1	AUC=0.48; p=0.603; pbonf=1
		Positive prediction error: pain relief	r(27)=-0.21; p=0.283; pbonf=1	AUC=0.48; p=0.592; pbonf=1
		Negative prediction error: pain relief	r(27)=-0.05; p=0.801; pbonf=1	AUC=0.50; p=0.500; pbonf=1
		US pain	r(27)=0.03; p=0.870; pbonf=1	AUC=0.51; p=0.469; pbonf=1
	Right nucleus accumbens	Anticipation money	r(27)=-0.11; p=0.586; pbonf=1	AUC=0.45; p=0.727; pbonf=1
		Anticipation pain relief	r(27)=0.35; p=0.060; pbonf=1	AUC=0.49; p=0.579; pbonf=1
		DS money	r(27)=0.13; p=0.516; pbonf=1	AUC=0.37; p=0.952; pbonf=1
		DS pain	r(27)=-0.22; p=0.242; pbonf=1	AUC=0.52; p=0.397; pbonf=1
		Positive prediction error: money	r(27)=0.16; p=0.396; pbonf=1	AUC=0.48; p=0.615; pbonf=1
		Negative prediction error: money	r(27)=-0.01; p=0.965; pbonf=1	AUC=0.42; p=0.864; pbonf=1
		Positive prediction error: pain relief	r(27)=0.09; p=0.655; pbonf=1	AUC=0.34; p=0.982; pbonf=1
		Negative prediction error: pain relief	r(27)=0.18; p=0.340; pbonf=1	AUC=0.42; p=0.850; pbonf=1
		US pain	r(27)=-0.37; p=0.049; pbonf=1	AUC=0.53; p=0.338; pbonf=1

Supplementary table 10: Alterations in fronto-striatal functional connectivity during reward learning is not associated with pain severity in patients with chronic back pain. Related to STAR Methods. The table shows correlations between the pain and the task-based functional connectivity between the ventromedial prefrontal cortex and bilateral nucleus accumbens during different learning processes. Parameter estimates were extracted from predefined masks extracted from neurosynth.org (see above), using a psychophysiological interaction (PPI) with the vmPFC as a seed region. Correlations are reported as Pearson's correlation with degrees of freedom (df), uncorrected p-values and Bonferroni-corrected p-values (corrected for 45 tests yielding a threshold of $p < 0.00111$). Additionally we created receiver operating characteristic (ROC) curves for classifying patients with chronic back pain and controls with the respective parameter estimates for fronto-striatal connectivity. We report the area under each ROC curve as an estimate of sensitivity and specificity. Associated p-values for the comparison to a chance-level ROC curve (i.e. AUC = 0.5) are reported as uncorrected p-values as well as Bonferroni-corrected p-values (corrected for 45 tests yielding a threshold of $p < 0.00111$). All results that survived the corrected statistical threshold ($p_{bonf} < 0.05$) are depicted in bold